

5-2019

# The Development of Screening Platforms to Identify Novel Anti-Infectives that Inhibit Protein Synthesis in *Pseudomonas aeruginosa*

Casey Anne Hughes  
*The University of Texas Rio Grande Valley*

Follow this and additional works at: <https://scholarworks.utrgv.edu/etd>



Part of the [Chemistry Commons](#)

---

## Recommended Citation

Hughes, Casey Anne, "The Development of Screening Platforms to Identify Novel Anti-Infectives that Inhibit Protein Synthesis in *Pseudomonas aeruginosa*" (2019). *Theses and Dissertations*. 479.  
<https://scholarworks.utrgv.edu/etd/479>

This Thesis is brought to you for free and open access by ScholarWorks @ UTRGV. It has been accepted for inclusion in Theses and Dissertations by an authorized administrator of ScholarWorks @ UTRGV. For more information, please contact [justin.white@utrgv.edu](mailto:justin.white@utrgv.edu), [william.flores01@utrgv.edu](mailto:william.flores01@utrgv.edu).

THE DEVELOPMENT OF SCREENING PLATFORMS TO IDENTIFY NOVEL  
ANTI-INFECTIVES THAT INHIBIT PROTEIN SYNTHESIS  
IN *PSEUDOMONAS AERUGINOSA*

A Thesis

by

CASEY ANNE HUGHES

Submitted to the Graduate College of  
The University of Texas Rio Grande Valley  
In partial fulfillment of the requirements for the degree of

MASTER OF SCIENCE

May 2019

Major Subject: Chemistry



THE DEVELOPMENT OF SCREENING PLATFORMS TO IDENTIFY NOVEL  
ANTI-INFECTIVES THAT INHIBIT PROTEIN SYNTHESIS  
IN *PSEUDOMONAS AERUGINOSA*

A Thesis  
by  
CASEY ANNE HUGHES

COMMITTEE MEMBERS

Dr. James Bullard  
Chair of Committee

Dr. Frank Dean  
Committee Member

Dr. Megan Keniry  
Committee Member

Dr. Evangelia Kotsikorou  
Committee Member

May 2019



Copyright 2019 Casey Anne Hughes

All Rights Reserved



## ABSTRACT

Hughes, Casey Anne., The Development of Screening Platforms to Identify Novel Anti-Infectives that Inhibit Protein Synthesis in *Pseudomonas aeruginosa*. Master of Science (MS), May 2019, 46 pp., 1 table, 23 figures, 41 references, 31 titles.

*Pseudomonas aeruginosa*, a Gram-negative opportunistic pathogen, is a leading cause of nosocomial infections and is becoming increasingly antibiotic resistant. Aminoacyl-tRNA synthetases (aaRSs) catalyze the covalent attachment of amino acids to their cognate tRNAs and serve as validated targets for the development of new anti-infectives. In *P. aeruginosa*, the genome contains two genes (*tyrS* and *tyrZ*) which encode two distinct TyrRS enzymes. The genes encoding both *P. aeruginosa* TyrRS-Z and TyrRS-S were cloned, overexpressed in *E. coli* cells, and purified to homogeneity. Both forms of TyrRS were active in aminoacylation and were developed into screening platforms using scintillation proximity assay (SPA) technology. Using this assay, a chemical compound library was screened to detect compounds with the ability to inhibit the function of TyrRS. A number of inhibitory compounds were confirmed and characterized for the ability to inhibit the enzymatic activity (IC<sub>50</sub>) of both forms of TyrRS.





## ACKNOWLEDGEMENTS

First of all, I am extremely grateful to my advisor, Dr. James Bullard, for giving me the opportunity to do research in his lab. I would like to thank him for his guidance, patience, and encouragement throughout my undergraduate and graduate years at UTRGV. He is an extraordinary mentor and provided an excellent atmosphere for performing research. I am very fortunate to have been a part of his lab.

My sincere thanks go to Dr. Frank Dean, Dr. Megan Keniry, and Dr. Evangelia Kotsikorou for serving on my thesis committee. I have greatly appreciated their help and encouragement.

I am also extremely thankful for the support of many lab members throughout the years who have assisted me in countless ways. Thanks to Samantha Balboa, Natalie Cantu, Varesh Gorabi, Yanmei Hu, Stephanie Palmer, Likhitha Aidunuthula, Humberto Salazar, Regina Zamacona, Sara Robles, Noah Pena, Beatriss Flores, and Maria Cavazos. It was a pleasure coming into work with such fun and encouraging people around.

A special thank you to Yaritza Escamilla for her friendship and support in research, coursework, and life.

Pursuing my education would have been difficult without the aid and support of my family. I am profoundly grateful for the love and encouragement they have given to me while I have been working towards my M.S. degree.

This work was supported by the National Institutes of Health (grant number 1SC3GM098173) to Dr. Bullard.



## TABLE OF CONTENTS

	Page
ABSTRACT .....	iii
ACKNOWLEDGEMENTS .....	iv
TABLE OF CONTENTS .....	v
LIST OF FIGURES .....	vii
CHAPTER I. INTRODUCTION .....	1
Antibiotic Resistance and <i>Pseudomonas aeruginosa</i> .....	1
Specific Mechanisms of Resistance .....	3
Protein Synthesis as a Target for Antibiotic Development .....	6
Tyrosyl-tRNA Synthetases .....	7
Scintillation Proximity Assay Technology .....	8
Testing Compounds Against PaPheRS, SpPheRS, and PaAspRS .....	8
The Use of Peptides as Antibiotics .....	9
CHAPTER II. METHODOLOGY .....	10
Tyrosyl tRNA Synthetases .....	10
Cloning, Expression, and Purification .....	10
Determination of Kinetic Parameters .....	12
Optimization of Screening Platform .....	13

Chemical Compound Screening: TyrRS .....	13
Glutamyl tRNA Synthetase .....	14
Chemical Compound Screening: GluRS .....	14
Testing Compounds against PaPheRS, SpPheRS, and PaAspRS .....	14
Testing Peptide against Protein Synthesis System .....	15
 CHAPTER III. RESULTS .....	 16
Tyrosyl tRNA Synthetases .....	16
Cloning, Expression, and Purification .....	16
Determination of Kinetic Parameters .....	20
Optimization of Screening Platforms .....	23
Chemical Compound Screening: TyrRS.....	26
Glutamyl tRNA Synthetase .....	33
Chemical Compound Screening: GluRS .....	33
Testing Compounds against PaPheRS, SpPheRS, and PaAspRS .....	37
Testing Peptide against Protein Synthesis System .....	39
 CHAPTER IV. CONCLUSION .....	 40
REFERENCES.....	42
BIOGRAPHICAL SKETCH.....	46

## LIST OF FIGURES

	Page
Figure 1: The development of new antibiotics versus increase of drug resistant bacteria.....	2
Figure 2: Alignment of PaTyrRS-S with the optimized PaTyrRS-S synthesized gene .....	17
Figure 3: Amino acid alignments of PaTyrRS-S: the native, planned optimized, and actual expressed synthesized protein sequence .....	18
Figure 4: Alignments of PaTyrRS-Z and PaTyrRS-S .....	18
Figure 5: Protein Purification and activity analysis of PaTyrRS-Z and PaTyrRS-S .....	19
Figure 6: Interactions of PaTyrRS-Z and PaTyrRS-S with ATP .....	21
Figure 7: Interactions of PaTyrRS-Z and PaTyrRS-S with tyrosine .....	21
Figure 8: Interactions of PaTyrRS-Z and PaTyrRS-S with tRNA <sup>Tyr</sup> .....	22
Figure 9: Optimizations of Components in Screening Platform with PaTyrRS-Z .....	24
Figure 10: Optimizations of Components in Screening Platform with PaTyrRS-S .....	25
Figure 11: Initial screen of the ChemDiv Soluble Diversity Library against the activity of PaTyrRS-Z and PaTyrRS-S.....	28
Figure 12: Confirmation of Initial Hit Compounds in Triplicate.....	29
Figure 13: Structure of the confirmed hit compound that inhibited PaTyrRS-Z .....	30
Figure 14: Structures of confirmed hit compounds that inhibited PaTyrRS-S .....	30
Figure 15: IC <sub>50</sub> determination for chemical compound tested with PaTyrRS-Z .....	31
Figure 16: IC <sub>50</sub> determination for chemical compounds tested with PaTyrRS-S .....	32
Figure 17: Initial screen of the ChemDiv Soluble Diversity Library against the activity of PaGluRS. ....	34

Figure 18: Confirmation of Initial Hit Compounds in Triplicate.....	35
Figure 19: Structures of confirmed hit compounds that inhibit PaGluRS .....	36
Figure 20: IC <sub>50</sub> plots of compounds against the activity of SpPheRS .....	37
Figure 21: IC <sub>50</sub> plots of compounds against the activity of PaPheRS .....	38
Figure 22: IC <sub>50</sub> plots of compounds against the activity of PaAspRS .....	38
Figure 23: Titration of the IF-1 peptide mimic into the aminoacylation/translation assay .....	39

## CHAPTER I

### INTRODUCTION

#### **Antibiotic Resistance and *Pseudomonas aeruginosa***

In recent years infectious diseases have become increasingly difficult to treat because bacteria are becoming more resistant to therapeutic remedies. Antibiotic resistance is a major global problem and has attracted significant media attention. In a report from the Centers for Disease Control and Prevention (CDC), it was estimated that at least 23,000 individuals die each year in the United States from pathogens exhibiting resistance to various antibiotics [1]. Commonly cited causes of this public health threat include misuse and overuse of antibacterials in the clinical and community setting, availability of non-prescription antibiotics in/from foreign countries, and widespread use of these drugs in livestock directly consumed by the human population [2]. At a molecular level, bacteria develop resistance through intrinsic and acquired mechanisms which are discussed in more detail below. Due to the exponential nature of bacterial reproduction, these processes, which lead to resistance, can occur very quickly. As certain bacteria become resistant to more than one drug, multidrug resistant “superbugs” are formed resulting in bacteria that have no known drugs to treat them [3]. According to the World Health Organization (WHO), research and development of antibiotics to combat these bacteria should be prioritized.

One pathogen of specific concern is *Pseudomonas aeruginosa*, an aerobic, Gram-negative bacteria that is a common cause of healthcare-associated infections including pneumonia, urinary



tract infections, and bloodstream infections [4] . In February 2017, this opportunistic pathogen was listed as “critical” and classified as one of the top three most threatening bacteria by the WHO [5]. The ability of this bacteria to form resilient biofilms on implanted medical devices, like catheters, as well as hospital surfaces and water sources, poses a problem because biofilms have the potential to become 10-1000 times more resistant than stand-alone bacteria [6]. This pathogen is especially life threatening to immunocompromised individuals due to *P. aeruginosa*'s high mortality rate. Cystic fibrosis (CF) patients are especially at risk because the pathogen forms biofilms in the lungs of these individuals leading to chronic pulmonary infections which is the leading cause of death in CF patients [7].

Although antibiotic resistance has become an increasing threat as current drugs become less effective, unfortunately, the research and development of new drugs to combat the problem has been dwindling [8]. In fact, the approval of new antibiotics by the FDA has been steadily decreasing since the 1980's (Fig. 1). This makes the discovery of new antibacterials especially crucial.

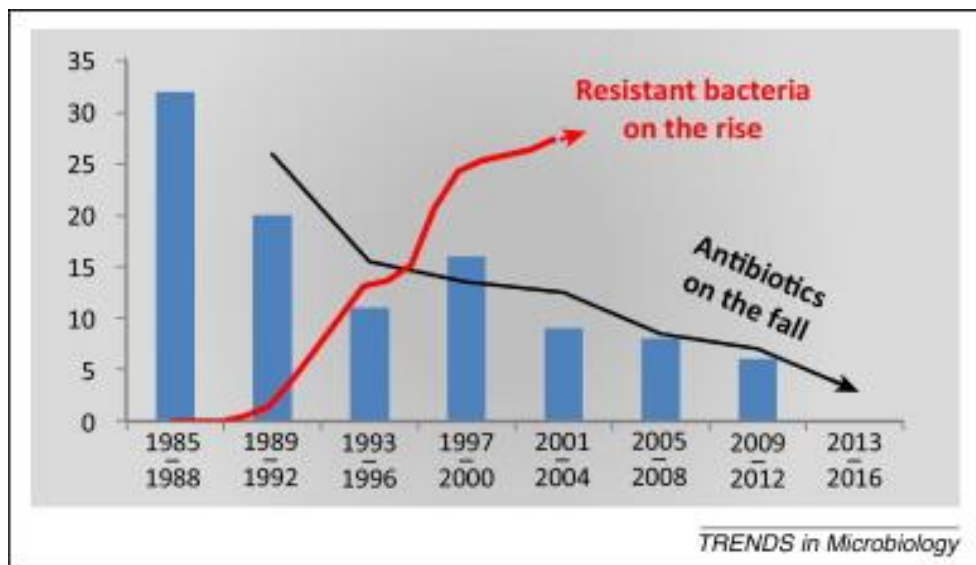


**Figure 1:** The development of new antibiotics versus increase of drug resistant bacteria [9]

## Specific Mechanisms of Resistance

At the molecular level, antibiotic resistance occurs through both intrinsic, acquired, and adaptive mechanisms. Intrinsic resistance is caused by multiple factors including the increasing existence of efflux pumps, reduced permeability of the bacterial cell membrane, and target site alteration which occurs through mutations in the binding site of the drug [10]. The resistance observed with *P. aeruginosa* is further increased by the pathogen's remarkable ability to acquire additional resistance mechanisms such as the uptake of resistance genes contained in foreign DNA via horizontal gene transfer through transduction, transformation, or conjugation [3]. When these mechanisms work together, this can lead to multidrug resistance. In addition to intrinsic and acquired resistance which frequently occurs, adaptive resistance, which involves bacteria becoming conditioned to antibiotics after repeated use, may play a role as well [11]. By understanding mechanisms of antibiotic resistance, drug developers are better able to design and/or discover potential anti-infectives.

Efflux is one of the most significant factors affecting microbial resistance. Efflux pumps are able to export dyes, detergents, inhibitors, disinfectants, organic solvents, and homoserine lactones as well as antibiotics from bacteria cells [12]. There are five different classes of efflux transporters that have been described in bacteria. These include the adenosine triphosphate (ATP)-binding cassette (ABC) family, the small multidrug resistance (SMR) family, the major facilitator superfamily (MFS), the multidrug and toxic compound extrusion (MATE) family, and the resistance nodulation division (RND) family [13]. The RND efflux family has been reported as the set of efflux pumps contributing the most to antimicrobial resistance in *P. aeruginosa* [14]. Many RND efflux transporters have been identified in *P. aeruginosa* and most of these transporters in Gram-negative bacteria are composed of three structures. This includes a transporter in the

cytoplasmic membrane, an outer membrane channel, and a periplasmic linker protein which connects those two structures [15]. This linker protein allows substrates to be released through bypassing the periplasm of the cell. The MexA-MexB-OprM, MexC-MexD-OprJ, MexE-MexF-OprN, and MexX-MexY-OprM multicomponent RND pump systems have been identified as playing the largest role in multidrug resistance because they have been identified in numerous clinical isolates [16]. Even though the RND systems are most prevalent, all five of these systems are able to individually remove multiple antibiotics that are commonly used to treat *P. aeruginosa* [17]. When more than one system is present in a bacterial strain, dual resistance further promotes antibiotic resistance [18]. While effective, these efflux systems have been shown to work slowly, and therefore reliance upon the outer membrane of the bacteria as a penetration barrier is also required to restrict anti-infectives from entering the cell [19, 20].

Three of the most administered anti-pseudomonal antibiotic classes are the fluoroquinolones, B-lactams, and aminoglycosides. The mechanisms of resistance in bacteria are known for these drugs [21]. In Gram-negative bacteria like *P. aeruginosa*, fluoroquinolones primarily function by binding to the  $\alpha$  subunit of DNA gyrase, and resistance often occurs through mutations in this enzyme [22]. In extremely resistant isolates, mutations may occur in topoisomerase IV (Topo IV) as well. Both of these proteins are made up of two subunits. Gyrase is composed of GyrA and GyrB while TopoIV contains ParC and ParE. Genes encoding GyrA and/or ParC are the genes where resistant mutations usually occur and are known as “quinolone resistance determining regions” (QRDR) [14]. The concerning phenomena of fluoroquinolone resistance is known by the acronym FQRP which stands for “fluoroquinolone resistant *P. aeruginosa*”.

Beta-lactam antibiotics target the synthesis of peptidoglycan in the bacterial cell wall. These broad-spectrum drugs contain a beta-lactam ring in their molecular structures and are deactivated by hydrolytic enzymes called beta-lactamases [23]. Beta-lactamase production has been cited as the main factor resulting in the acquired resistance to beta-lactam antibiotics in *P. aeruginosa* [24]. These enzymes disrupt the amide bond in the beta-lactam ring which causes the drug to be ineffective. There are four different classes of these enzymes which include metal dependent and metal independent beta-lactamases. Class A, C, and D are characterized via a serine based mechanism while the Class B enzymes, known as metallo-beta-lactamases, require zinc [25]. All four classes are found in *P. aeruginosa*. Carbapenems, a specific type of beta-lactam antibiotic, are able to resist most beta-lactamases due to a unique fused beta-lactam ring structure [26]. Because of this property, these drugs are used in the treatment of MDR infections. However, even carbapenems are becoming less effective against *P. aeruginosa* due to mutations in the OprD outer membrane porin protein which is the main entry site for these drugs [27].

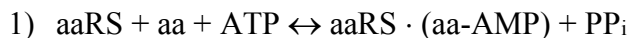
Aminoglycosides target protein synthesis by binding to the 30S subunit of the bacterial ribosome, inducing codon misreading and inhibition of translocation [26]. Bacteria exhibit resistance to these antibiotics primarily due to aminoglycoside modifying enzymes (AME's), rRNA methylases, and endogenous efflux mechanisms [24]. AME's include aminoglycoside phosphoryltransferases, aminoglycoside acetyltransferases, and aminoglycoside nucleotidyltransferases which phosphorylate, acetylate, or adenylate the aminoglycoside respectively and reduce the binding affinity of the drug for the 30S subunit [28]. Resistance to some aminoglycosides such as gentamicin, tobramycin, and amikacin results from methylation of the 16S rRNA of the 30S subunit of the ribosome by 16S rRNA methylases. The aminoglycoside class of antibiotics is frequently used to treat infections in the airways of cystic fibrosis patients.

Tobramycin has specifically had success by inhalation through nebulization [29]. In many clinical isolates from cystic fibrosis patients, the MexXY-OprM multidrug resistant efflux system has also been shown to affect the efficacy of aminoglycosides [24].

### **Protein Synthesis as a Target for Antibiotic Development**

Protein synthesis is an essential metabolic process which occurs in all bacteria and blocking this process kills or retards growth of the pathogen, resulting in either a bactericidal or bacteriostatic global mode of inhibition. There are three stages in protein synthesis which can be specifically targeted: initiation, elongation, and termination. In addition to the ribosome, the proteins involved in initiation of protein synthesis are the initiation factors (IF-1, IF-2, IF-3) and methionyl-tRNA formyltransferase (MFT). The elongation phase of protein synthesis requires the elongation factors (EF-Tu, EF-Ts, EF-G). This stage also involves aminoacylation, or charging, of the tRNA, with a specific (cognate) amino acid which is then transported to the ribosome during protein synthesis for insertion into a growing nascent peptide. The attachment of the amino acid to the cognate tRNA is catalyzed by a group of enzymes, the aminoacyl-tRNA synthetases (aaRS). Finally, termination and recycling uses the release factors (RF1, RF2, RF3) to end protein synthesis and recycle the components of the translational complex once this complex encounters a stop codon in the messenger RNA (mRNA).

AaRS enzymes have been shown to be valid targets for antibiotic development [30]. These enzymes function by attaching amino acids to their cognate tRNAs before delivery to the ribosome during protein biosynthesis. This process occurs via a two-step esterification reaction, where in the first step an aminoacyl-adenylate intermediate (aa-AMP) is formed and in the second step the amino acid is transferred to the 2'- or 3'- hydroxyl group of the terminal adenosine of tRNA [31].



Because divergence of the primary amino acid sequence has occurred between prokaryotic and eukaryotic aaRS, drugs can be identified that selectively target bacterial enzymes without inhibiting the corresponding human enzymes [30]. Since each amino acid has a corresponding tRNA synthetase, there are many different targets to explore. For example, one current antibiotic on the market, Mupirocin, targets the isoleucyl-tRNA synthetase.

### Tyrosyl tRNA Synthetases

In bacteria, there are two classes of tyrosyl-tRNA synthetases, TyrRZ and TyrRS [32]. *P. aeruginosa*, unlike most bacteria, has both synthetases, one encoded by the *tyrZ* gene and one encoded by the *tyrS* gene (PaTyrRS-Z and PaTyrRS-S). These enzymes are both classified as Class 1 aaRS which are characterized by the presence of two consensus sequences in the active site region, HIGH and KMSKS, and the binding of ATP which occurs in the Rossmann fold catalytic domain. They are further classified as Class 1c enzymes due to their similar subunit structure [33].

The attachment of correct amino acids to the corresponding cognate tRNAs is vital for the fidelity of protein synthesis, a process known as tRNA identity. While several aaRS have various fidelity mechanisms to ensure accuracy, the tyrosyl tRNA synthetases have no difficulty discriminating between amino acids and therefore have no independent editing domains [34].

This project involved cloning, expressing, and purifying PaTyrRS-Z and PaTyrRS-S. After purification, the enzymes were characterized and the kinetic parameters governing the interactions with the natural substrates were determined. Next, aminoacylation assays for each enzyme were optimized and converted to a high throughput format. These screening platforms

were then used to screen chemical compound libraries to identify compounds that inhibit protein synthesis in *P. aeruginosa*.

### **Scintillation Proximity Assay Technology**

The screening platform developed to identify inhibitors of protein synthesis utilizes scintillation proximity assay (SPA) technology. This radioisotopic assay is able to rapidly and sensitively measure aminoacylation of tRNA, making it a viable option for high throughput screening [35]. Assay reaction mixtures contain necessary components for aminoacylation including radiolabeled amino acids, the cognate tRNA, and the catalyzing specific enzyme. After the reaction is completed it is stopped by the addition of ethylenediaminetetraacetic acid (EDTA). To monitor the level of activity of aminoacylation, yttrium silicate (YSi) poly-L-lysine coated beads are added to the stopped reaction. Under acidic conditions, these SPA beads bind to the tRNA. The tRNA that were aminoacylated with a radioactive amino acid is thus placed in close proximity to the beads. The radioisotopic decay of the radioactive amino acid emits  $\beta$  particles which stimulates the scintillant within the beads to emit light that is recognized by a PMT based scintillation counter [36].

### **Testing Compounds against PaPheRS, SpPheRS, and PaAspRS**

Structure based drug development is another strategy in antibiotic discovery. Computational methods may be used to identify inhibitors of essential enzymes in bacteria. Comparative structure modeling is used to develop 3D structures of various enzymes using Molecular Operating Environment (MOE) Software. Compounds developed using this process by Dr. Claire Simon's laboratory (Cardiff University, UK) were tested against the purified phenylalanyl-tRNA synthetases from *S. pneumonia* and *P. aeruginosa* as well as the *P. aeruginosa* aspartyl-tRNA synthetase. Compounds were serially diluted and tested against aminoacylation

assays to establish IC<sub>50</sub> values of the compounds and determine if the compounds were able to inhibit enzymatic function.

### **The Use of Peptides as Antibiotics**

An additional strategy for developing antimicrobials involves the use of peptides as antibiotics [37]. As part of this project, a peptide synthesized in Dr. Yonghong Zhang's lab (UTRGV) was tested using a polyU mRNA-directed aminoacylation/translation (A/T) assay [38]. At concentrations elevated above the physiological concentration, If-1 blocks binding of the 50S ribosomal subunit to the 30S initiation complex thus blocking protein synthesis. The peptide was designed to block IF-1 from binding to the ribosome and therefore "unblock" binding of the 50S ribosomal subunit and allowing protein synthesis to continue. To test the peptide, it was titrated into the A/T Assay to determine if it could relieve the inhibitory activity of elevated levels of IF-1 in the *P. aeruginosa* protein synthesis system.



## CHAPTER II

### METHODOLOGY

#### Tyrosyl-tRNA Synthetases

##### Cloning, Expression, and Purification

The gene encoding *P. aeruginosa* TyrRS-Z was amplified using PCR (MJ Mini Thermo Cycler, Bio-Rad, Hercules, CA) using *P. aeruginosa* PAO1 genomic DNA (ATCC 47085) as a template. A forward primer (5'-TAACGCTAGCAAATCGGTTGAAGAGCAGCT-3') and a reverse primer (5'-CTCTAAGCTTTTCAGCTTTCAGCGTGATG-3') were used to add *Nhe*I and *Hind*III restriction sites to the ends of the gene. The amplified gene was inserted into pET24b(+) plasmid (Novagen) which was also digested with *Nhe*I/*Hind*III restriction enzymes forming pET-PaTyrZ.

pET-PaTyrZ was transformed into *E. coli* Rosetta 2 (DE3) Singles Competent Cells and cultures were grown in Terrific Broth (TB). The broth contained 50 µg/mL of kanamycin and 25µg/mL of chloramphenicol and was grown at 37° C to an optical density ( $A_{600}$ ) of 0.6-0.8. Overexpression of TyrRS-Z was then induced by addition of isopropyl β-D-1-thiogalactopyranoside (IPTG) to 500 µM. Growth was continued for 3 hours post-induction and the bacteria were harvested by centrifugation (10,000 g, 4 °C, 45 min).

Amplification of TyrRS-S by PCR was unsuccessful, therefore the gene sequence was optimized for codon expression and synthetically synthesized by Integrated DNA Technologies

(IDT). The plasmid containing the synthesized *tyrS* gene was digested with *NheI* and *HindIII* and the fragment was inserted into the pET24b(+) plasmid (Novagen) which had also been digested with *NheI/HindIII* restriction enzymes, forming pET-PaTyrS. The recombinant plasmid was then transformed into *E. coli* Rosetta 2 (DE3) Singles Competent Cells and cultures were grown in Luria Burtani (LB) broth containing 50 µg/mL of kanamycin and 25µg/mL of chloramphenicol at 25 °C until an optical density ( $A_{600}$ ) of 0.6-0.8 was reached. Overexpression of TyrRS-S was induced by addition of IPTG to 25 µM. Bacteria was grown for five hours post-induction and harvested by centrifugation (10,000 g, 4 °C, 45 min).

Fraction 1 lysates of both proteins were prepared as previously explained [39]. Purification of *P. aeruginosa* TyrRS-Z was achieved by precipitation of the protein in a solution containing 50% saturated ammonium sulfate (AS) while *P. aeruginosa* TyrRS-S was precipitated in a 60% AS solution. Both PaTyrRS-Z and PaTyrRS-S were purified to greater than 95% homogeneity using nickel nitrilotriacetic acid (NTA) affinity chromatography (Perfect Pro, 5 Prime) followed by dialysis (two times) against a buffer containing: 20 mM Hepes-KOH (pH 7.0), 40 mM KCl, 1 mM MgCl<sub>2</sub>, 0.1 mM EDTA, 10 % glycerol. Purified proteins were flash frozen in liquid nitrogen and stored at -80 °C. Concentrations were determined by the Bradford method using Coomassie Protein Assay Reagent (Thermo Scientific, Waltham, MA). Sodium dodecyl sulfate-polyacrylamide gel electrophoresis (SDS-PAGE) was performed using 4-12% polyacrylamide precast gels (Novex NuPAGE; Invitrogen, Grand Island, NY) with 3-(N-morpholino)propanesulfonic acid (MOPS) running buffer (Invitrogen). EZ-Run Rec Protein Ladder was utilized as a protein standard (Fisher Scientific). Gels were stained using Simply Blue Safe Stain (Invitrogen).

## Determination of Enzymatic Kinetic Parameters

**Timed tRNA Aminoacylation Assays:** Timed aminoacylation reactions were measured using scintillation proximity assay (SPA) technology. Reactions were 50  $\mu\text{L}$  and carried out in a 96 well plates (costar). A master mix was created which resulted in the final reaction containing 50 mM Tris-HCl (pH 7.5), 10 mM  $\text{MgCl}_2$ , 2.5 mM ATP, 0.5 mM Spermine, 75  $\mu\text{M}$  [ $^3\text{H}$ ] tyrosine, 1 mM dithiothreitol (DTT) and either 0.0015  $\mu\text{M}$  PaTyrRS-Z or 0.05  $\mu\text{M}$  PaTyrRS-S. To start the reactions, tRNA was added to the master mix and incubated at 37  $^\circ\text{C}$ . The tRNA concentrations were varied in seven different sets of assays and contained 10, 20, 30, 40, 50, 60, and 70  $\mu\text{M}$  total tRNA (0.16, 0.32, 0.48, 0.64, 0.8, 0.96  $\mu\text{M}$  tRNA<sup>tyr</sup>). Reactions were stopped after 1, 2, 3, 4, and 5 minute intervals by the addition of 5  $\mu\text{L}$  of 0.5 M EDTA. Four hundred micrograms of yttrium silicate (Ysi) poly-L-Lysine-coated SPA beads (Perkin Elmer) in 150  $\mu\text{L}$  of 300 mM citric acid (pH 2.0) were added and allowed to incubate at room temperature for 1 h. The plates were analyzed using a 1450 Microbeta (Jet) liquid scintillation/luminescent counter (Wallac). From these assays, initial velocities were measured and the kinetic parameters ( $K_M$ ,  $V_{\text{max}}$ , and  $k_{\text{cat}}$ ) were established by fitting the data to the Michaelis-Menten steady-state model using XLfit (IBDS).

**Phosphate Exchange Reactions:** ATP:PP<sub>i</sub> exchange reactions (100  $\mu\text{L}$ ) were carried out in 50 mM Tris-HCl (pH 7.5), 10 mM KF, 8 mM  $\text{MgCl}_2$ , 1 mM DTT, 2 mM [ $^{32}\text{P}$ ]PP<sub>i</sub> (50 cpm/pmol) and contained 0.4  $\mu\text{M}$  of either PaTyrRS-Z or PaTyrRS-S. Reactions were incubated at 37 $^\circ\text{C}$  for 1, 2, 3, 4, and 5 minutes. In reactions in which the concentration of ATP was varied (50, 100, 200, 300, 400, 500, 600, and 700  $\mu\text{M}$ ), the amino acid tyrosine (Tyr) remained constant at 2 mM; alternatively, when the concentration of Tyr was varied (12.5, 25, 50, 100, 200, 250  $\mu\text{M}$ ), the ATP concentration remained at 2 mM. The exchange of PP<sub>i</sub> in these reactions was measured between one and five min. Reactions were stopped by immediately spotting 5  $\mu\text{L}$  of the reaction solution

onto PEI cellulose TLC plates (Selecto Scientific). ATP and  $PP_i$  were separated using a solution containing 4 M urea and 0.75 M  $KP_i$  (pH 3.5) as a mobile phase [40]. Amounts of ATP,  $PP_i$  and  $P_i$  were quantified using a Typhoon FLA 7000 Laser Scanner (GE Healthcare). Initial velocities for exchange of  $PP_i$  were determined and the kinetic parameters ( $K_M$ ,  $V_{max}$ , and  $k_{cat}$ ) for the interactions of TyrRS-Z and TyrRS-S with ATP and tyrosine were determined by plotting the velocities against substrate concentration and fit to the Michaelis-Menten steady-state model using XLfit (IDBS).

### **Optimization of Screening Platform**

Multiple titrations were performed to determine the optimal concentrations of several reactants used in screening assays. The concentrations of  $MgCl_2$ , Spermine, DMSO, and EDTA were optimized in assays for both PaTyrRS-Z and PaTyrRS-S. The reactant being tested was varied in concentration while the other components were held at constant concentration. Non-titrated components included 50 mM Tris HCl, 2.5 mM ATP, 75  $\mu$ M [ $^3H$ ] tyrosine, and 1 mM DTT. Reactions were performed in SPA format and were stopped and analyzed as described above for timed aminoacylation assays.

### **Chemical Compound Screening: TyrRS**

The Soluble Diversity chemical compound library from ChemDiv, Inc. was screened against the activity of the TyrRS enzymes. SPA technology was used to monitor tRNA aminoacylation. Reactions were performed in 96 well plates as described above in the timed aminoacylation assay. 33  $\mu$ L of protein/master mix containing 0.1  $\mu$ M of either PaTyrRS-Z or PaTyrRS-S was mixed with 2  $\mu$ L test compounds (3.3 mM) dissolved in 100% DMSO. Positive controls for both enzymes contained 2  $\mu$ L of DMSO in the absence of compound. Negative controls for PaTyrRS-Z contained the master mix with no enzyme. Negative controls for

PaTyrRS-S contained 10  $\mu$ L of EDTA. Reactions were incubated for 15 min at room temperature before being initiated by addition of 15  $\mu$ l of *E. coli* tRNA<sup>Tyr</sup> (54  $\mu$ M), followed by incubation and analysis. Compounds which inhibited 50% of enzymatic activity were considered initial hits. Assays to confirm these compounds were carried out in triplicate as described above. Assays to determine IC<sub>50</sub> values were also performed as described above except the test compounds were serially diluted from 400  $\mu$ M to 0.4  $\mu$ M.

### **Glutamyl-tRNA Synthetases**

#### **Chemical Compound Screening: GluRS**

PaGluRS was previously cloned, expressed, and purified. The enzyme was used in the chemical compound screening of the ChemDiv Soluble Diversity Library as described above for PaTyrRS-Z and PaTyrRS-S. Positive controls contained 2  $\mu$ L of DMSO and negative controls contained 2  $\mu$ L EDTA. Confirmation assays were performed in triplicate.

#### **Testing Compounds against PaPheRS, SpPheRS, and PaAspRS**

A set of 52 compounds received from Dr. Claire Simon's laboratory at Cardiff University were dissolved in DMSO and serially diluted into SPA assays at concentrations from 200-0.4  $\mu$ M. Assays were performed to determine IC<sub>50</sub> values for the compounds against *P. aeruginosa* PheRS and *S. pneumoniae* PheRS which had been previously purified in our laboratory. The concentrations of the enzymes were 0.8 and 0.2  $\mu$ M respectively. The tRNA<sup>Phe</sup> concentration was 29  $\mu$ M per reaction.

A set of 29 compounds also from Dr. Simon's laboratory were tested against *P. aeruginosa* AspRS to determine IC<sub>50</sub> values as described above for PheRS. *P. aeruginosa* AspRS had also

been previously purified and characterized in our laboratory. The enzyme concentration was 0.025  $\mu\text{M}$  and 54  $\mu\text{M}$  of tRNA<sup>Asp</sup> was used per reaction.

### **Testing Peptide against Protein Synthesis System**

The peptide tested from Dr. Zhang's laboratory was dissolved in DMSO and serially diluted at concentrations from 200-0.4  $\mu\text{M}$  for use in aminoacylation/translation (A/T) assay [41]. Assay master mix contained 50 mM Tris-HCl (pH 7.5), 0.1  $\mu\text{M}$  *P. aeruginosa* ribosomes, 10 mM MgCl<sub>2</sub>, 25 mM KCl, 4 mM PEP, 0.025 U/ $\mu\text{L}$  PK, 1.5 mM ATP, 0.5 mM GTP, 40  $\mu\text{M}$  [<sup>3</sup>H] phenylalanine, 0.3 mg/ml polyU RNA, 0.65  $\mu\text{M}$  *P. aeruginosa* EF-TU, 0.2  $\mu\text{M}$  *P. aeruginosa* EF-G #2, 0.03  $\mu\text{M}$  spermine, 1 mM DTT, 0.1  $\mu\text{M}$  *P. aeruginosa* PheRS, 10  $\mu\text{M}$  IF-3 and 5  $\mu\text{M}$  IF-1. Reactions were initiated by the addition of 32.3  $\mu\text{M}$  tRNA and incubated at 37 °C for 1 h. Next, assays were stopped by the addition of 5  $\mu\text{L}$  of 0.5 M EDTA. A mixture of 148  $\mu\text{l}$  300 mM citrate buffer (pH 6.2) and 2  $\mu\text{l}$  RNA binding beads (YSi; Perkin-Elmer) were added. Plate was analyzed 24 h later in a 1450 Microbeta (Jet) liquid scintillation/luminescent counter (Wallac).

## CHAPTER III

### RESULTS

#### Tyrosyl-tRNA Synthetases

##### Cloning, Expression, and Purification

PaTyrRS-Z was cloned using normal methods starting with amplification of the TyrRS-Z gene by PCR. Although multiple sets of primers were designed with different lengths for various regions around the gene, amplification of TyrRS-S by PCR was unsuccessful. Therefore, the *tyrS* gene sequence was optimized for codon expression and synthetically synthesized (Fig. 2). Alteration of the gene did not affect the amino acid sequence of the translated protein as shown in Figure 3. An alignment of PaTyrRS-Z and PaTyrRS-S shows that the proteins are 41.4% conserved and 26.8% identical (Fig. 4).

Both PaTyrRS-Z and PaTyrRS-S were overexpressed in *E. coli* and purified to greater than 95% homogeneity as visualized by SDS-PAGE (Fig. 5A). Titrations of both proteins into aminoacylation assays showed that the enzymes were active (Fig. 5B, and Fig. 5C).

		1		75
Pa TyrRS (tyrS)	(1)	-----GTTTCCTCCCGACCCATCAGCAAGACCTGATCGCCCTGCTCGAAGAAGGTGGCTTCCTCCACCG		
Pa TyrRS-S gene rebuilt	(1)	-----ATGTCCTGTCCCGACTCATCAGCAAGACTTATGGCTCTGCTGGAAGAAGTGGTTTTGTACATCAA		
		76		150
Pa TyrRS (tyrS)	(67)	TGCACCGACCTGCACCGCCTTCCGCGGCACTGGCCGCCGGTCCGGCAACCGCTACCTGGGCCTCAGCSCAAC		
Pa TyrRS-S gene rebuilt	(67)	TGACTGATCGTGAAGTCTTGTGCTCATCTTGTGCTGGTCCGCAACTGCTTACCTGGGTTTGATGCTAG		
		151		225
Pa TyrRS (tyrS)	(142)	GCCGACAGCCTGGACGTCGGCCACTACAGGGCTGATGCTGATGCCCTGGCTACAAGAGCCGGGACCCGCCG		
Pa TyrRS-S gene rebuilt	(142)	GCTGATCTCTTCAATGTAAGTCACTTCAAGGCTTATGCTATGCCCTGGCTCAAAAAGCTGGTCAACCTCT		
		226		300
Pa TyrRS (tyrS)	(217)	TGCTGCTGATCGGTGGCCGACCGCGATCGCCGATCCGAGCTTCCCGATTGAGCCGGCCGATCCTCAC		
Pa TyrRS-S gene rebuilt	(217)	TGCTGCTGATGGTGGTGGTACACTCGTATTGGTATCCAGCTTCCGATTGAGTGGTCTATCTGAT		
		301		375
Pa TyrRS (tyrS)	(292)	GAGGCGCAGATCCAGGCCAACATCGACCGCATCGCCGGGTTTTCTCCGCTACCTCGAACTGCACGACGAC		
Pa TyrRS-S gene rebuilt	(292)	GAGCTCAGATCAAGCTAACATCGATGGTATGCTCGTATTCTCCGTTAGTGAAGCTGATGATCT		
		376		450
Pa TyrRS (tyrS)	(367)	CTGGTGAAACAAGCCCAATGGCTGGACGGCTCGGCACCTGAGTTCCTCGACCGGTCCGGCCGACTTCTG		
Pa TyrRS-S gene rebuilt	(367)	CTGGTTAAACAAGCTCAATGGCTGATGCTGTGGTACCTGAGTTCCTGATCGTGTGGTCACTTCT		
		451		525
Pa TyrRS (tyrS)	(442)	ATCAACCGCTGCTGACTTCGACCGCATCAGCAGCGCTTGGACCGCGAGCATTGGTCTGCTTCTCGATT		
Pa TyrRS-S gene rebuilt	(442)	ATCAACCGCTGCTGACTTCGATGCTATCCGTCAGCGCTTGGACCGTGAACATTCTGCTTCTCGATT		
		526		600
Pa TyrRS (tyrS)	(517)	GGCTACACCCTGCTGCAAGCCTACGATTTTCGTGAACTGTCCGCGCCCGCTGACACTGCGCACTCCG		
Pa TyrRS-S gene rebuilt	(517)	GGCTACACTGCTGCAAGCCTACGATTTTCGTGAACTGTCCGTCCTGCTGCTGCACTGCGCACTGGTGG		
		601		675
Pa TyrRS (tyrS)	(592)	GCCGACCAATGGGCAACATCATCAACGGCTGGAGGTGTGAGACCGAGGGCCGCGCCAGCTGTTCCGCTG		
Pa TyrRS-S gene rebuilt	(592)	GCTGATCAATGGGCAACATCATCAACGGTGTGAGGTGTCCGTCGTCAGGCTGGTGCCTGCTGTTGGCTG		
		676		750
Pa TyrRS (tyrS)	(667)	ACCATGCCCTGCTGGCCACAGTGAAGGCGCAAGATGGCAAGTGGGCAAGGTGGCGTATGGCTCAACGCC		
Pa TyrRS-S gene rebuilt	(667)	ACCATGCCCTGCTGGCTACCTGTGATGGTCGAAGATGGCAAGTGGTGCACAGGTGCTATGGCTGAACGG		
		751		825
Pa TyrRS (tyrS)	(742)	GAGGCTGCGGCGCCTTCGACTTCTGGCAGTCTGGCCCAACTGCSATGATCCGACCTCGGTCCCTTCTCC		
Pa TyrRS-S gene rebuilt	(742)	GACGCTGCGGCTCGTTCGACTTCTGGCAGTCTGGCCCAACTGCSATGATCCGATGATGGTCTTCTCC		
		826		900
Pa TyrRS (tyrS)	(817)	CTGTTACGCAACTGCCGATGGATGAGGTGGCGCCCTGGCCGCTTGCAGGGCGCCGAGCTGAACGAAGCAAG		
Pa TyrRS-S gene rebuilt	(817)	CTGTTACGCAACTGCCATGGATGAGTACGTCGTGGGCTGCCTGCAAGGCTGATGAACGAAGCAAG		
		901		975
Pa TyrRS (tyrS)	(892)	GTGGTCTGGCCAAATGCCCGCACCGCCTGGCGCACGGCGAACAAGTCCGCGCCGATGCCCGCCCG		
Pa TyrRS-S gene rebuilt	(892)	GTGGTCTGGCAATGCCCGTACACTGGCCATGGTGAACATCGCTGCTGCTGATGCCCTGCT		
		976		1050
Pa TyrRS (tyrS)	(967)	GGGGTCTTCGCCCAAGTACCGGGACAGCGCCCTGGCCGTGATGAAGCTATCCGCGCGCCCTGGCCGAGGA		
Pa TyrRS-S gene rebuilt	(967)	GGGTAATCGCCAAAGTACCTGACTCTGGCTGGCCGTGATGAAGCTGCTCGTCTGCTGCTGATGCCCTG		
		1051		1125
Pa TyrRS (tyrS)	(1042)	CTGTCTGCTGACCGACTGCTGCTGGAACAACCGATCCAGCCCTCCGCGAGCGCGGTCTGCGCCCTCC		
Pa TyrRS-S gene rebuilt	(1042)	CTGTCTGCTGACTGATCTGCTGCTGGAACAACCGATCCAGCCCTCCGCGAGCGCGGTCTGCGCCCTCC		
		1126		1200
Pa TyrRS (tyrS)	(1117)	GGCGGCTGCGCCTGGACCGCAAGCCGGTTCAGCGATCCGGACAGCCGCTGGGGGGCGAGTTCGACGGCTG		
Pa TyrRS-S gene rebuilt	(1117)	GGTGGTCTGGCTGGATGGTACCTGGTTCAGCGATCCGGACAGCCGCTGGCTGGTGAAGTGAAGTCTGG		
		1201		1251
Pa TyrRS (tyrS)	(1192)	TTGAGCCTGGCAAGAAGCAGCATTTGCACCTGCGACTCGAGGATTCG		
Pa TyrRS-S gene rebuilt	(1192)	TGAGCCTGGCAAGAAGCAGCATTTGCACCTGCGCTCTGAGGATTCG		

**Figure 2:** Alignment of PaTyrRS-S with the optimized PaTyrRS-S gene that was synthesized. Nucleotides shown with blue background indicate the nucleotides changed in the optimized gene sequence.



			1		75
	Pa TyrRS-S	(1)	--	MSVPTHQQDLIALLEERG	FVHQCTDRDGLAAHLAAGPATAYLGF
Translation of IDT synthesized Pa tyrS gene		(1)	MAS	SVPTHQQDLIALLEERG	FVHQCTDRDGLAAHLAAGPATAYLGF
Translation of Pa TyrRS-S gene rebuilt		(1)	--	MSVPTHQQDLIALLEERG	FVHQCTDRDGLAAHLAAGPATAYLGF
			76		150
	Pa TyrRS-S	(74)	LLIGGAT	TRIGDPSFRDSSRPILTEAQIQANIDGIARVFSRYVELHDDSLVNNAEWL	DGVGYLEFLDRVGRHFSI
Translation of IDT synthesized Pa tyrS gene		(76)	LLIGGAT	TRIGDPSFRDSSRPILTEAQIQANIDGIARVFSRYVELHDDSLVNNAEWL	DGVGYLEFLDRVGRHFSI
Translation of Pa TyrRS-S gene rebuilt		(74)	LLIGGAT	TRIGDPSFRDSSRPILTEAQIQANIDGIARVFSRYVELHDDSLVNNAEWL	DGVGYLEFLDRVGRHFSI
			151		225
	Pa TyrRS-S	(149)	NRLT	TFDAIRQRDLREHSLSFLEFGYTLQAYDFVELSRRRGCTLQGGADQWANIINGVELSRRQGG	AQLFGLT
Translation of IDT synthesized Pa tyrS gene		(151)	NRLT	TFDAIRQRDLREHSLSFLEFGYTLQAYDFVELSRRRGCTLQGGADQWANIINGVELSRRQGG	AQLFGLT
Translation of Pa TyrRS-S gene rebuilt		(149)	NRLT	TFDAIRQRDLREHSLSFLEFGYTLQAYDFVELSRRRGCTLQGGADQWANIINGVELSRRQGG	AQLFGLT
			226		300
	Pa TyrRS-S	(224)	MPLLATS	DGRKMGKSAQGA	VAVLN
Translation of IDT synthesized Pa tyrS gene		(226)	MPLLATS	DGRKMGKSAQGA	VAVLN
Translation of Pa TyrRS-S gene rebuilt		(224)	MPLLATS	DGRKMGKSAQGA	VAVLN
			301		375
	Pa TyrRS-S	(299)	VLANA	TALAHGEHAARS	AADAARGVFADGTRD
Translation of IDT synthesized Pa tyrS gene		(301)	VLANA	TALAHGEHAARS	AADAARGVFADGTRD
Translation of Pa TyrRS-S gene rebuilt		(299)	VLANA	TALAHGEHAARS	AADAARGVFADGTRD
			376		416
	Pa TyrRS-S	(374)	GLRLD	GTFVSDPDTPLAGEVDGLRSLGKKQHLHLRLED	--
Translation of IDT synthesized Pa tyrS gene		(376)	GLRLD	GTFVSDPDTPLAGEVDGLRSLGKKQHLHLRLED	KL
Translation of Pa TyrRS-S gene rebuilt		(374)	GLRLD	GTFVSDPDTPLAGEVDGLRSLGKKQHLHLRLED	--

**Figure 3:** Amino acid alignments of PaTyrRS-S: the native, the planned optimized, and actual expressed synthesized protein sequence.

			1		100
Pa TyrRS-S	(1)	MSVPTHQQDLIALLEERG	FVHQCTDRDGLAAHLAAGPATAYLGF	DATA	DSLHVGH
Pa TyrRS-Z	(1)	---MKSVEQLALIQRC	ADEILVEALWAKLKR	QGLRIKAGFP	PTAPDLHLGH
			101		200
Pa TyrRS-S	(101)	QANIDGIARVFSRYVELHDDSLVNNAEWL	DGVGYLEFLDRVGRHFSINRLITF	DAIRQLDREHSLSFLEFGYTLQAYDFVELSRRRGCTLQGGADQ	
Pa TyrRS-Z	(97)	LENASTYKSQVFKILDP	PAKTEAFNSTWMDQTPA	PIFRLASQYTVARMLERD	DFSKRYASNQPTA
			201		300
Pa TyrRS-S	(201)	WANLINGVELSRRQGG	AQLFGLTMPLLATS	DGRKMGKSAQGA	VAVLN
Pa TyrRS-Z	(192)	KFNLMGRELQRAYQ	QEAQVILTMPLLEGLD	GVKMSKILGN	YIGIQEAPGVM
			301		400
Pa TyrRS-S	(299)	VLANA	TALAHGEHAARS	AADAARGVFADGTRD	SGLPVMKLSR
Pa TyrRS-Z	(290)	KLAE	EIVARFHGE	AAA	SAHKSAGNRLK
			401		414
Pa TyrRS-S	(399)	SLGKKQHHLRLED			
Pa TyrRS-Z	(387)	GKKA	FAR	THLAE	

**Figure 4:** Alignments of PaTyrRS-Z and PaTyrRS-S. Amino acids in yellow are conserved (identical) while amino acids in green are similar. The sequences are 41.4% conserved and 26.8% identical.

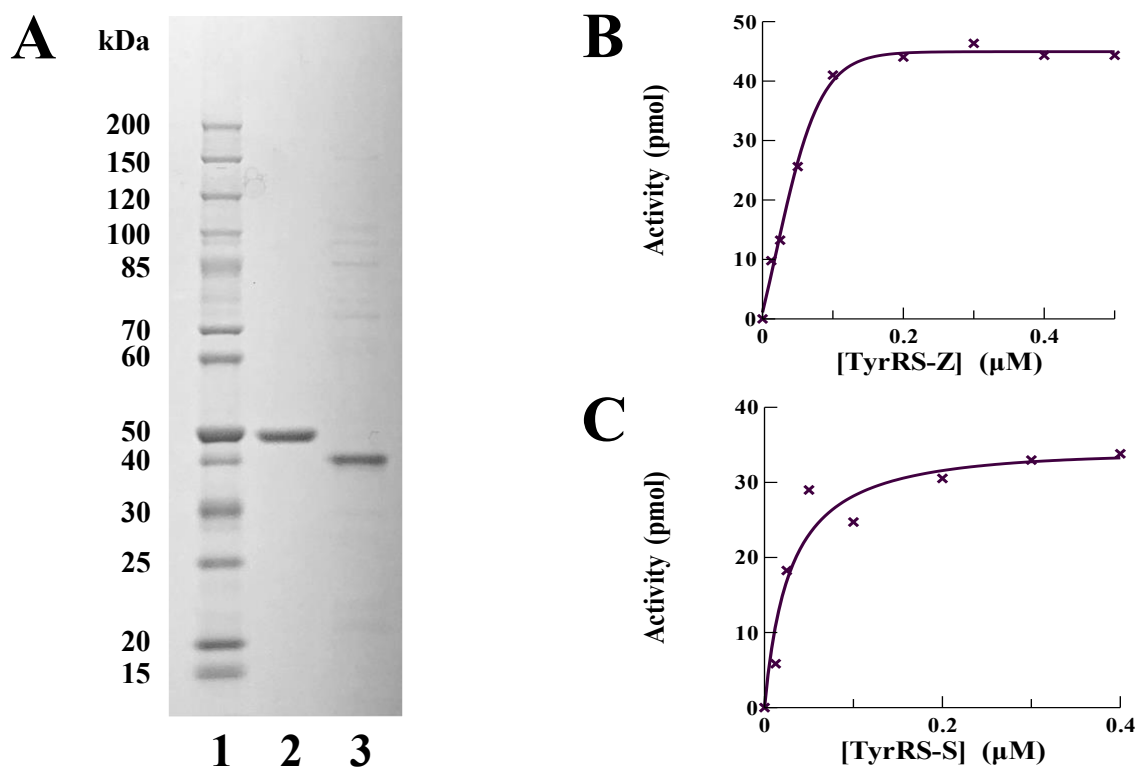


**Figure 5:** Protein purification and activity analysis of PaTyrRS-Z and PaTyrRS-S. A) SDS-page gel containing the following: 1. Ladder; 2. PaTyrRS-Z (2  $\mu\text{g}$ ; 48.7 kDa); 3. PaTyrRS-S (2  $\mu\text{g}$ ; 46.8 kDa). B) Titration of PaTyrRS-Z into aminoacylation assay. C) Titration of PaTyrRS-S into aminoacylation assay.

## Determination of Enzymatic Kinetic Parameters

Aminoacyl tRNA synthetases function by catalyzing the attachment of the amino acid to its cognate tRNA through a two-step reaction. The first step of the reaction results in the formation of an aminoacyl adenylate and release of inorganic pyrophosphate. When tRNA isn't present, the reaction becomes reversible and can be used to observe the interaction of the enzymes with ATP and amino acid. Using the ATP:PP<sub>i</sub> exchange assay, the interactions of PaTyrRS-Z and PaTyrRS-S with ATP and tyrosine were monitored as described in the "Methods" section. The kinetic parameters,  $K_M$ ,  $V_{max}$ ,  $k_{cat}$ , and  $k_{cat}/K_M$  governing the interaction of PaTyrRS-Z with ATP were determined to be 496  $\mu\text{M}$ , 92  $\mu\text{M}/\text{min}$ , 3.8  $\text{s}^{-1}$ , and 0.008  $\text{s}^{-1} \text{uM}^{-1}$ , respectively (Fig. 7A). For interactions with tyrosine, the same kinetic parameters were 29  $\mu\text{M}$ , 75  $\mu\text{M}/\text{min}$ , 3.1  $\text{s}^{-1}$ , and 0.11  $\text{s}^{-1} \text{uM}^{-1}$ , respectively (Fig. 8A). The kinetic parameters,  $K_M$ ,  $V_{max}$ ,  $k_{cat}$ , and  $k_{cat}/K_M$ , for interactions of PaTyrRS-S with ATP were 204  $\mu\text{M}$ , 24  $\mu\text{M}/\text{min}$ , 1  $\text{s}^{-1}$ , and 0.005  $\text{s}^{-1} \text{uM}^{-1}$ , respectively, (Fig. 7B) while those values for interaction with tyrosine were 172  $\mu\text{M}$ , 91  $\mu\text{M}/\text{min}$ , 3.8  $\text{s}^{-1}$ , and 0.022  $\text{s}^{-1} \mu\text{M}^{-1}$  (Fig. 8B).

The second step of this reaction involves the transfer of the amino acid from aminoacyl adenylate to tRNA and can be monitored using timed aminoacylation assays. Using this method, the kinetic parameters  $K_M$ ,  $V_{max}$ ,  $k_{cat}$ , and  $k_{cat}/K_M$  were determined to be 2.1  $\mu\text{M}$ , 0.17  $\mu\text{M}/\text{min}$ , 1.9  $\text{s}^{-1}$ , 0.9  $\text{s}^{-1} \mu\text{M}^{-1}$ , respectively, for PaTyrRS-Z and 0.81  $\mu\text{M}$ , 0.26  $\mu\text{M}/\text{min}$ , 0.086  $\text{s}^{-1}$ , and 0.11  $\text{s}^{-1} \mu\text{M}^{-1}$  for PaTyrRS-S.

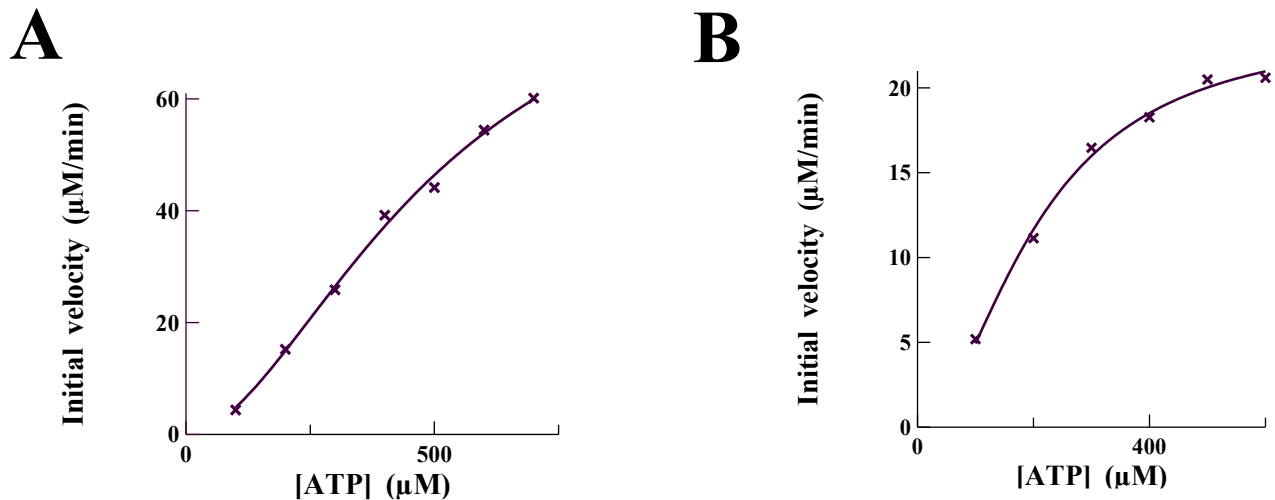


**Figure 6:** Interactions of A) PaTyrRS-Z and B) PaTyrRS-S with ATP. ATP:PP<sub>i</sub> exchange assays were used to determine the enzymatic kinetic parameters ( $K_M$ ,  $V_{max}$ , and  $k_{cat}$ ) for interactions with ATP.

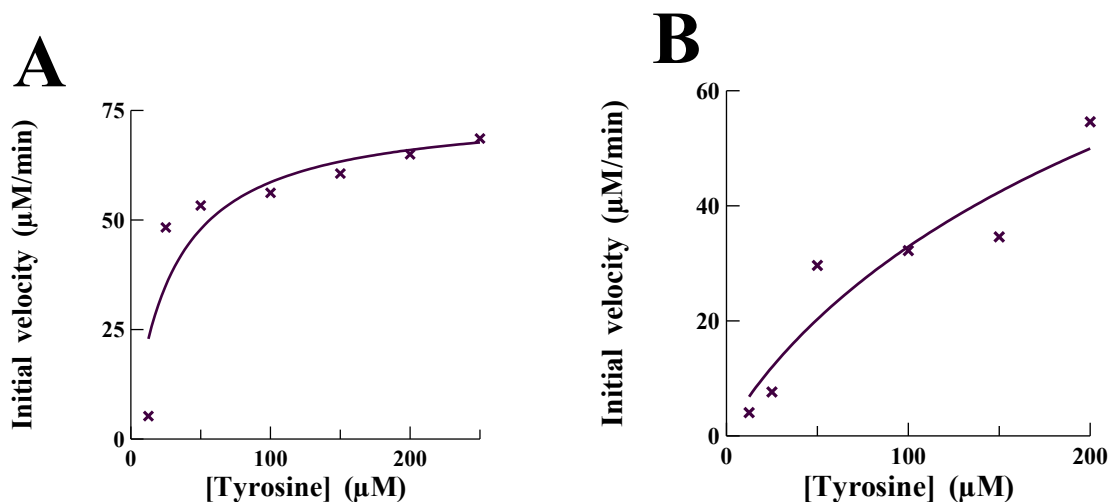


**Figure 7:** Interactions of A) PaTyrRS-Z and B) PaTyrRS-S with tyrosine. ATP:PP<sub>i</sub> exchange assays were used to determine the enzymatic kinetic parameters ( $K_M$ ,  $V_{max}$ , and  $k_{cat}$ ) for interactions with tyrosine.

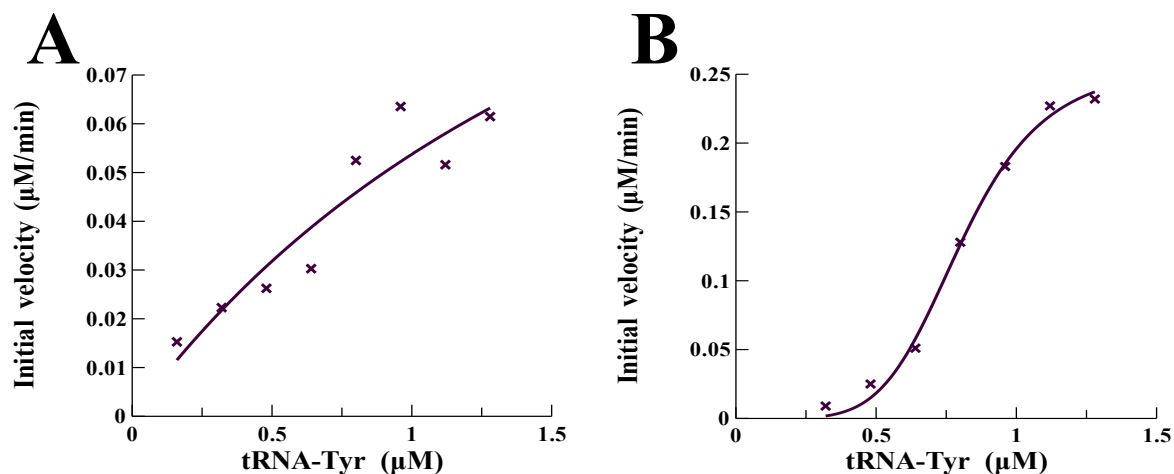


**Figure 8:** Interactions of A) PaTyrRS-Z and B) PaTyrRS-S with tRNA<sup>Tyr</sup>. Aminoacylation assays were used to determine the enzymatic kinetic parameters ( $K_M$ ,  $V_{max}$ , and  $k_{cat}$ ) for interactions with tRNA.

	PaTyrRS-Z			PaTyrRS-S		
	Tyrosine	ATP	tRNA	Tyrosine	ATP	tRNA
$K_M$ ( $\mu\text{M}$ )	29	496	2.1	172	204	0.81
$V_{max}$ ( $\mu\text{M}/\text{min}$ )	75	92	0.17	91	24	0.26
$k_{cat}$ ( $\text{s}^{-1}$ )	3.1	3.8	1.9	3.8	1	0.086
$k_{cat}/K_M$ ( $\text{s}^{-1} \text{uM}^{-1}$ )	0.11	0.008	0.9	0.022	0.005	0.11

**Table 1:** Summary of kinetic parameters describing the interactions of PaTyrRS-Z and PaTyrRS-S with the three substrates.

## Optimization of the Screening Platform

Multiple components of the aminoacylation screening assay were titrated separately into the assay to determine optimal concentrations for maximum activity. First, PaTyrRS-Z and PaTyrRS-S were individually titrated (Fig. 5B-C). Next, tRNA, MgCl<sub>2</sub>, and spermine were titrated in assays containing PaTyrRS-Z or PaTyrRS-S (Fig. 9-10). The optimal concentrations of tRNA, MgCl<sub>2</sub>, and spermine were determined to be 53.76 μM, 10 mM, and 0.5 mM respectively in both PaTyrRS-Z and PaTyrRS-S assays. Since chemical compounds were dissolved in 100% DMSO, resulting in final DMSO concentrations in screening assays of 4%, the ability of *P. aeruginosa* PaTyrRS-S and PaTyrRS-Z to function in the presence of increasing amounts of DMSO was determined. There was no loss of activity due to DMSO at concentrations up to 10% DMSO observed.

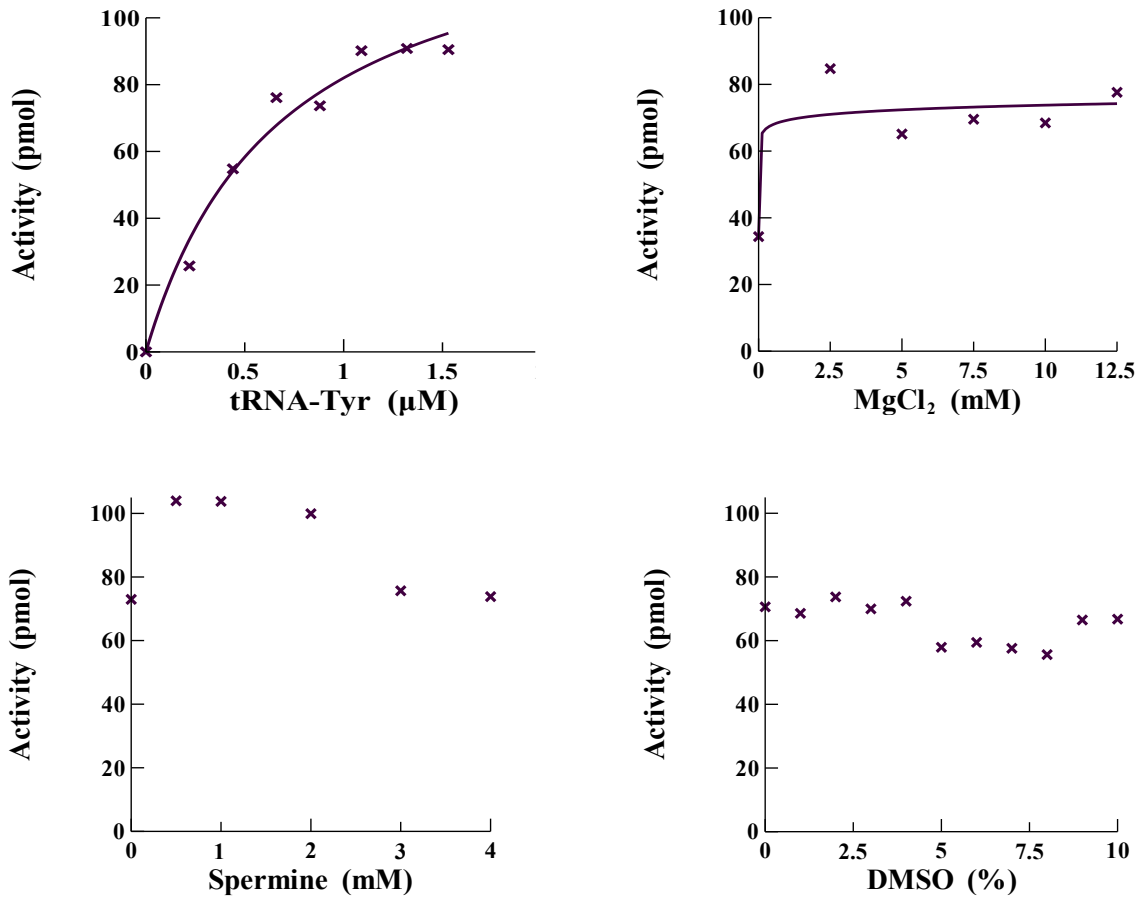


**Figure 9:** Optimizations of Components in Screening Platform with PaTyrRS-Z

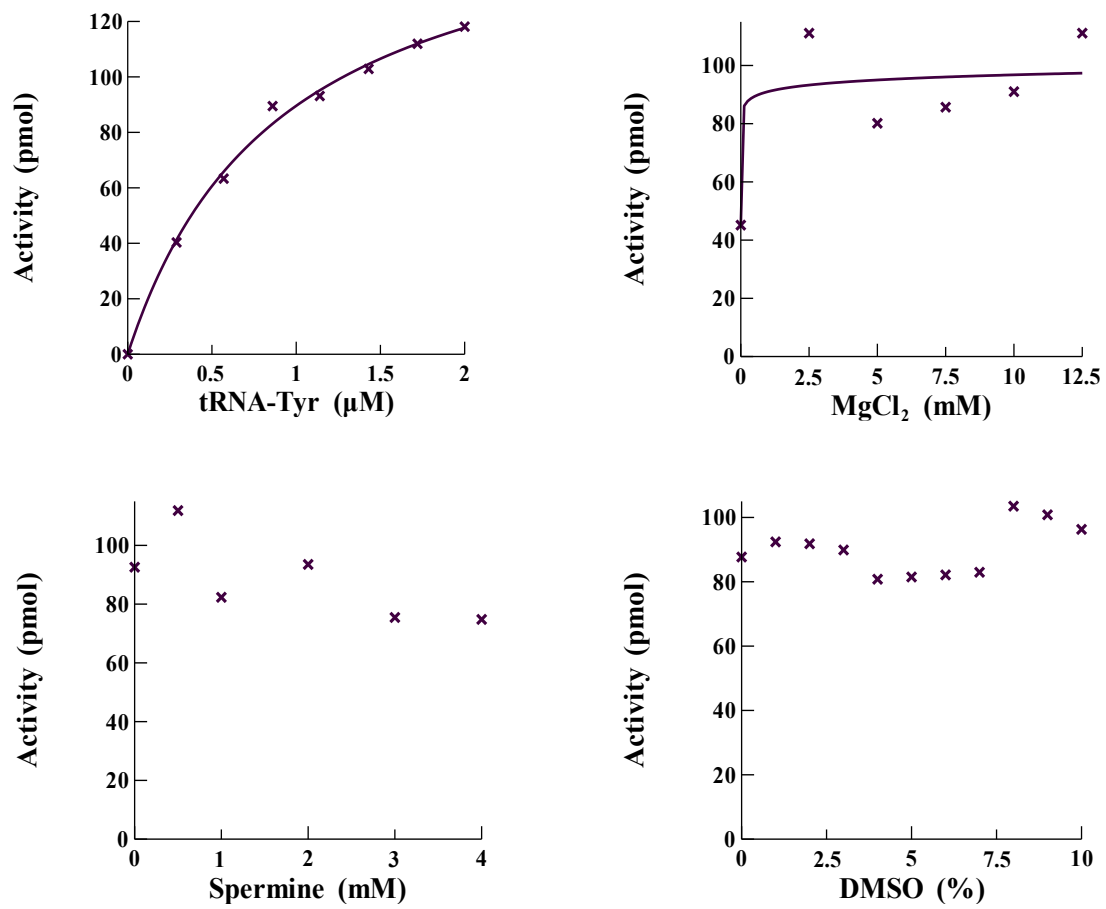


**Figure 10:** Optimizations of Components in Screening Platform with PaTyrRS-S



## Chemical Compound Screening: TyrRS

The ChemDiv Soluble Diversity Library, containing 2000 compounds, was screened for inhibitory activity using PaTyrRS-Z and PaTyrRS-S screening platforms as described in “Materials and Methods”. Positive controls for both screening platforms contained two  $\mu\text{L}$  of DMSO in the absence of compound (Fig. 11A-B, column 1 A-D and column 12 E-H). For PaTyrRS-Z, the negative control contained master mix with no enzyme (Fig. 11B, column 1 E-H and column 12 A-D). A minus enzyme control was carried out because EDTA failed to inhibit the reaction at acceptable levels. For the screen against the activity of PaTyrRS-S, ten  $\mu\text{L}$  of EDTA was used to inhibit activity and used as a negative control (Fig. 11A, column 1, E-H and column 12 A-D). Results were converted to percent positive and plotted using 3-D scatter graph (JMP Pro 14). Compounds were considered initial hits if 50% of the activity was inhibited. From the initial screens, 16 compounds were identified that inhibited PaTyrRS-Z and out of these compounds, one compound was confirmed to have inhibitory activity (Fig. 12A and 13). Thirty compounds were identified that inhibited PaTyrRS-S and 10 compounds were confirmed to have inhibitory activity (Fig. 12B and 14). Structural analysis was performed and of these 10 compounds, five were identified for additional analysis. The compound that inhibited enzymatic activity of PaTyrRS-Z was also a confirmed hit compound for PaTyrRS-S (Fig. 13 and Fig. 14B).

$\text{IC}_{50}$  assays were performed with the one confirmed compound for PaTyrRS-Z and the five compounds for PaTyrRS-S as described in “Materials and Methods”. Reactions were carried out to determine the compound concentration that inhibited 50% of the activity of the reaction. The data was analyzed using XL fit (Version 5.1; IDBS) as part of Microsoft Excel (Fig. 15 and 16). BCD38C11, the compound that confirmed for PaTyrRS-Z had an  $\text{IC}_{50}$  value of 269  $\mu\text{M}$ . The five

compounds tested against PaTyrRS-S, BCD37H6, BCD38C11, BCD49D9, BCD50C3, BCD54B4 and BCD59D9 had IC<sub>50</sub> values of 23.68, 71.90, 65.9, 39.0, and 44.31  $\mu$ M respectively.

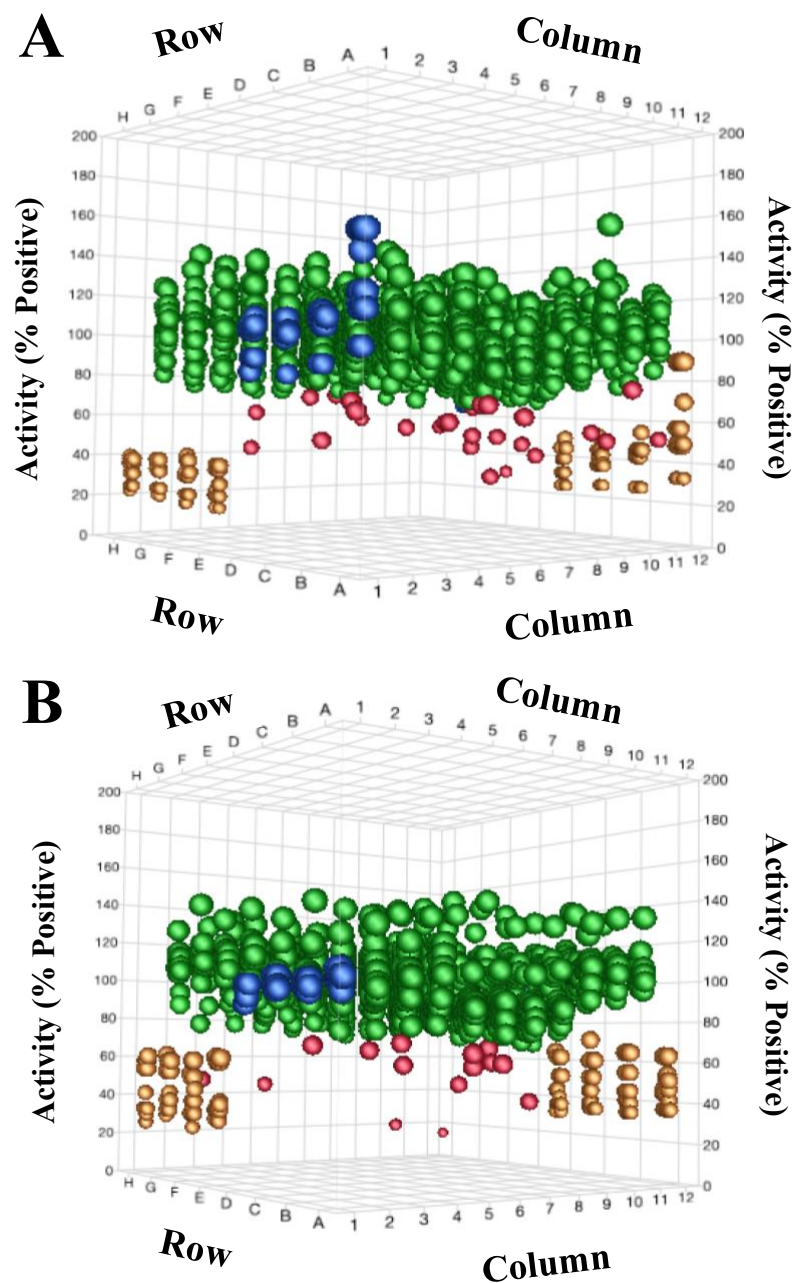


**Figure 11:** Initial screen of the ChemDiv Soluble Diversity Library against the activity of PaTyrRS-Z and PaTyrRS-S. A) Results from the PaTyrRS-Z screen; B) Results from the TyrRS-S screen. The graph depicts the DMSO positive control (blue spheres), EDTA negative control (yellow spheres), primary hits (red spheres), and compounds that did not inhibit enzymatic activity (green spheres).

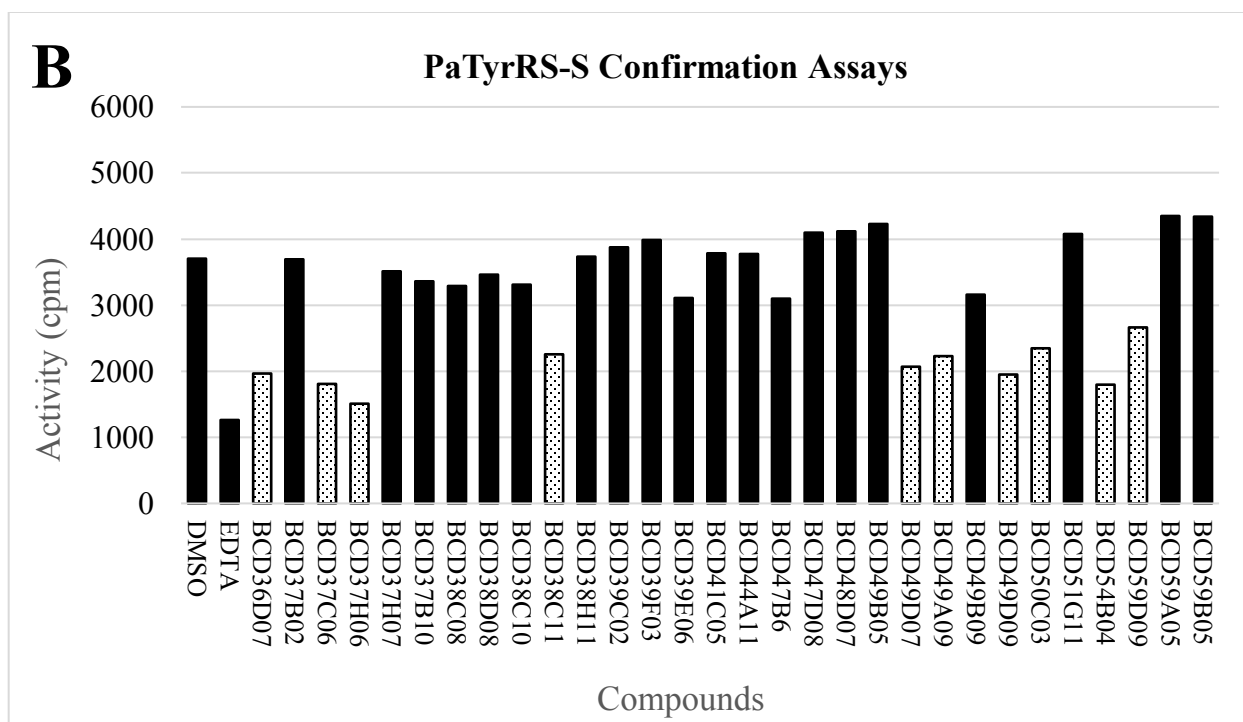
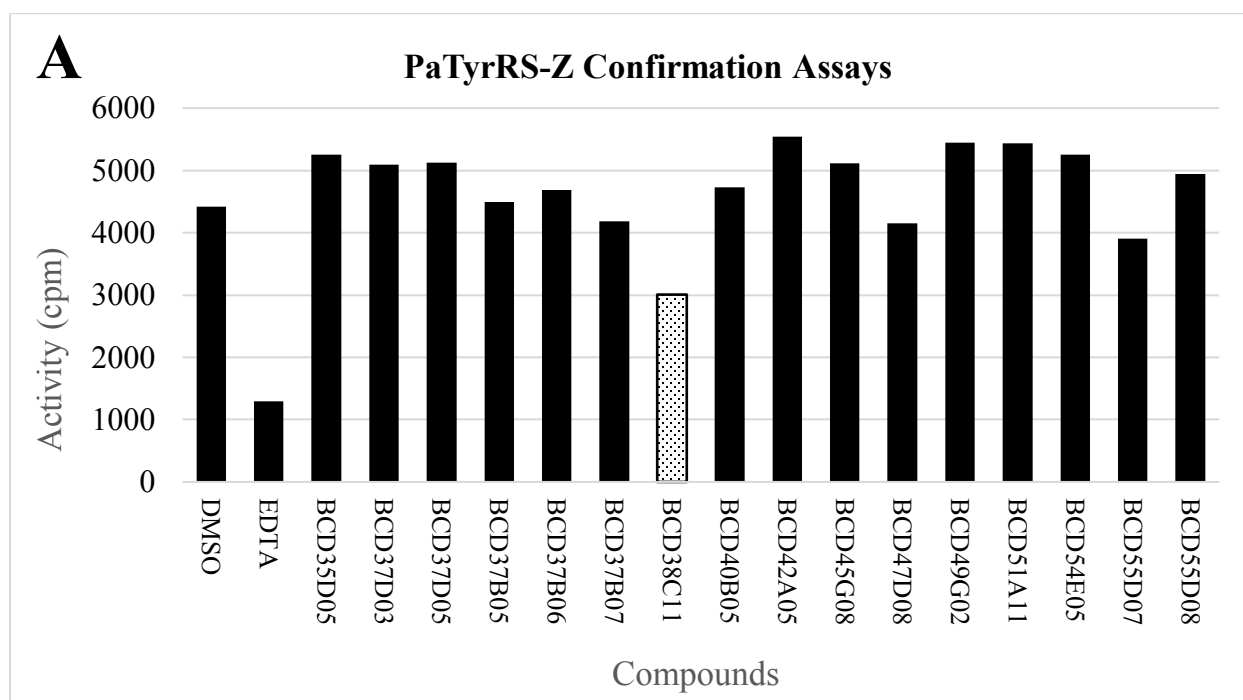


**Figure 12:** Confirmation of the inhibitory activity of the initial hit compounds carried out in triplicate assays. The hits that were confirmed are denoted by dotted pattern.

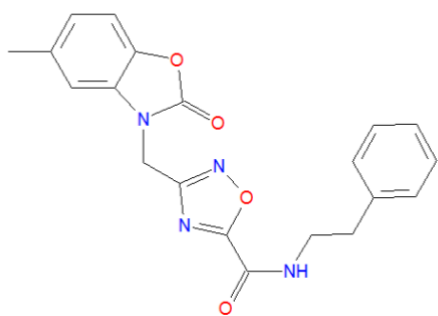


**Figure 13:** Structure of the confirmed hit compound BCD38C11 that inhibits enzymatic activity of PaTyrRS-Z

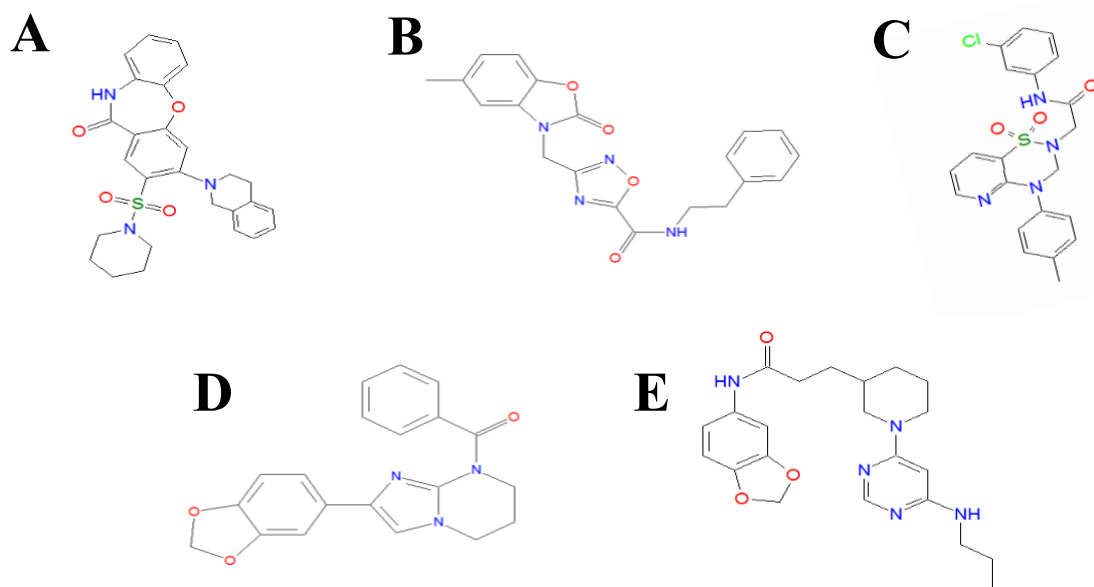


**Figure 14:** Structures of confirmed hit compounds that inhibited the enzymatic activity of PaTyrRS-S. A) BCD37H06; B) BCD38C11; C) BCD49D09; D) BCD50C03; E) BCD54B04.

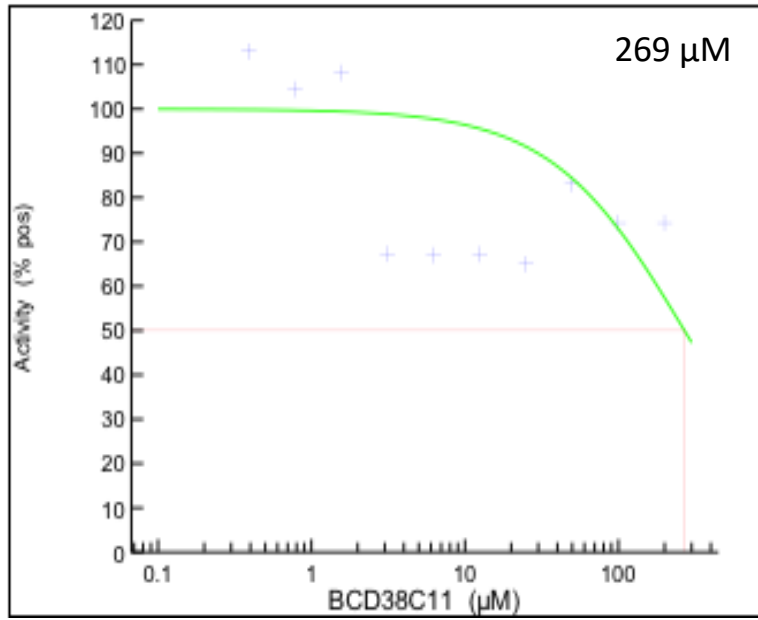


**Figure 15:** IC<sub>50</sub> determination for chemical compound BCD38C11 tested with PaTyrRS-Z.

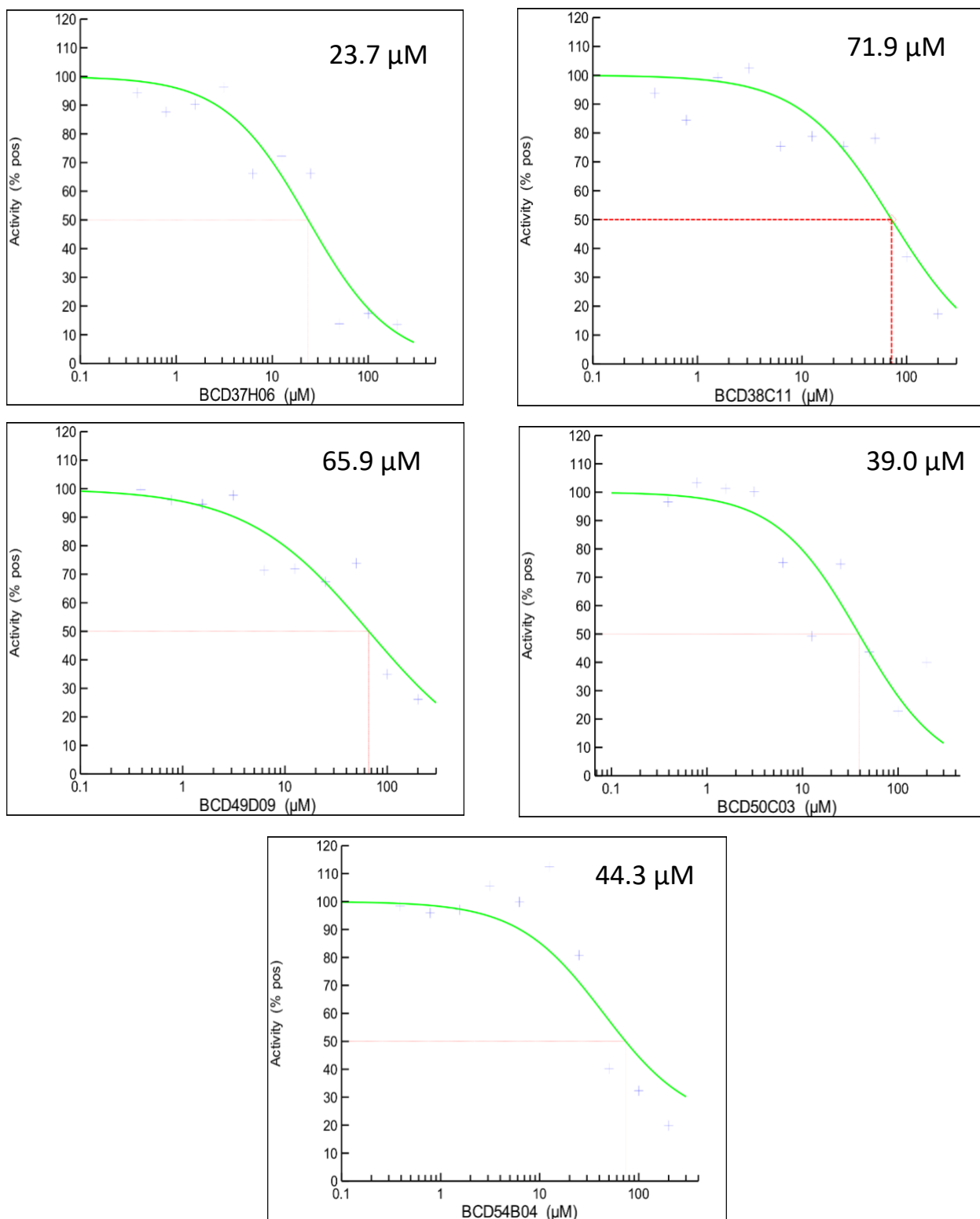


**Figure 16:** IC<sub>50</sub> determination for chemical compounds BCD37H6, BCD38C11, BCD49D9, BCD50C3 and BCD54B4 tested with PaTyrRS-S.

## Glutamyl-tRNA Synthetase

### Chemical Compound Screening: GluRS

The ChemDiv Soluble Diversity Library containing 2000 compounds was screened against the activity of *P. aeruginosa* GluRS as described in “Materials and Methods”. Positive controls contained two uL of DMSO in the absence of compound (Fig. 15, column 1 A-D and column 12 E-H). Negative controls contained two uL of EDTA (Fig. 15, column 1, E-H and column 12 A-D). Results were converted to percent positive and plotted using 3-D scatter graph (JMP Pro 14). Compounds were considered initial hits if 50% of the activity was inhibited. From the initial screens, 32 compounds were identified that inhibited PaGluRS and 17 compounds were confirmed to have inhibitory activity. Structural analysis was performed and of these 17 compounds, eight compounds were identified for additional analysis (Fig.17).



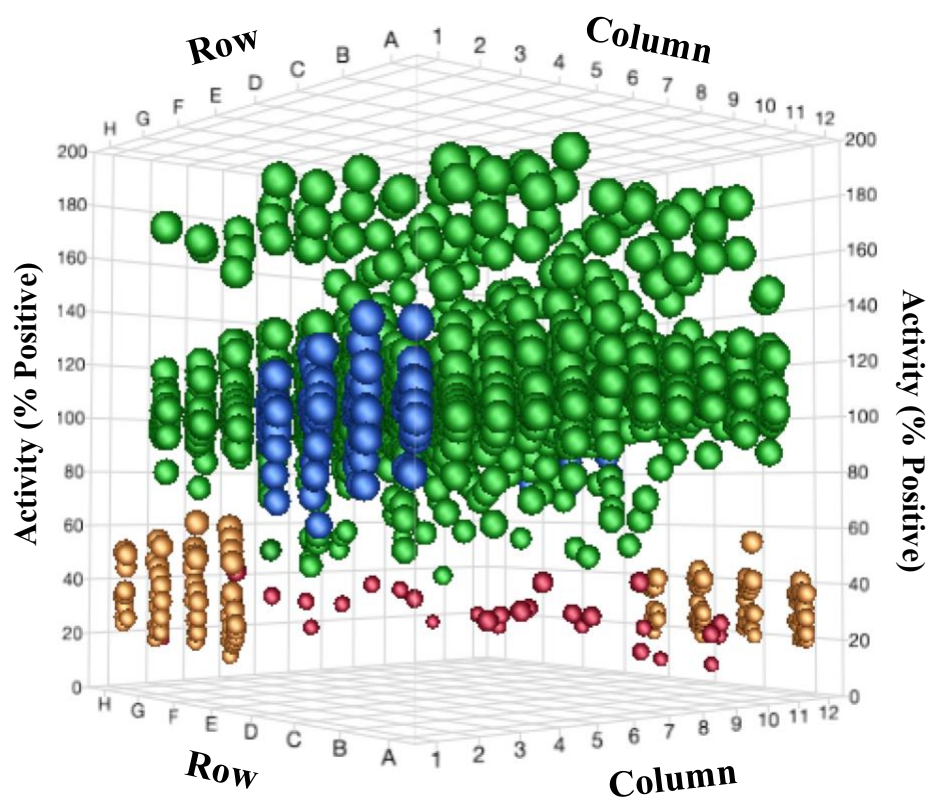


**Figure 17:** Initial screen of the ChemDiv Soluble Diversity Library against the activity of PaGluRS. The graph depicts the DMSO control (blue spheres), EDTA control (yellow spheres), primary hits (red spheres), and compounds that did not inhibit enzymatic activity (green spheres).

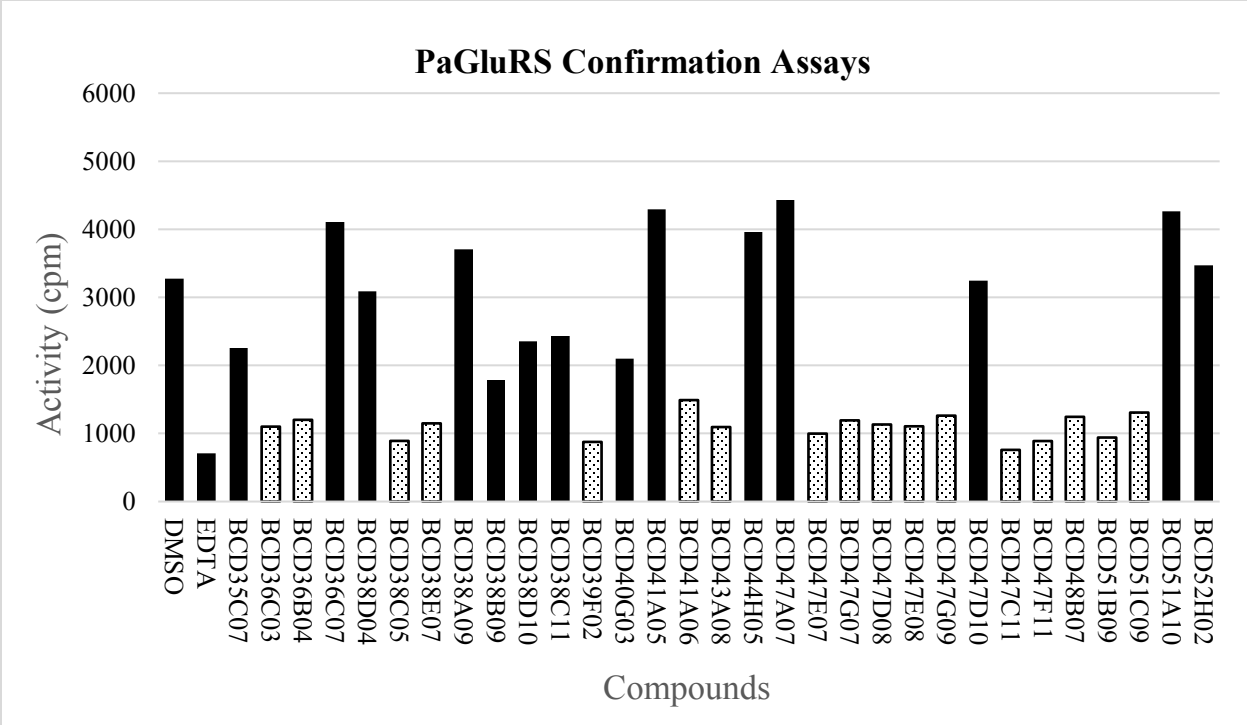


**Figure 18:** Confirmation of the initial hit compounds carried out in triplicate assays. Confirmed hits are denoted by dotted pattern.

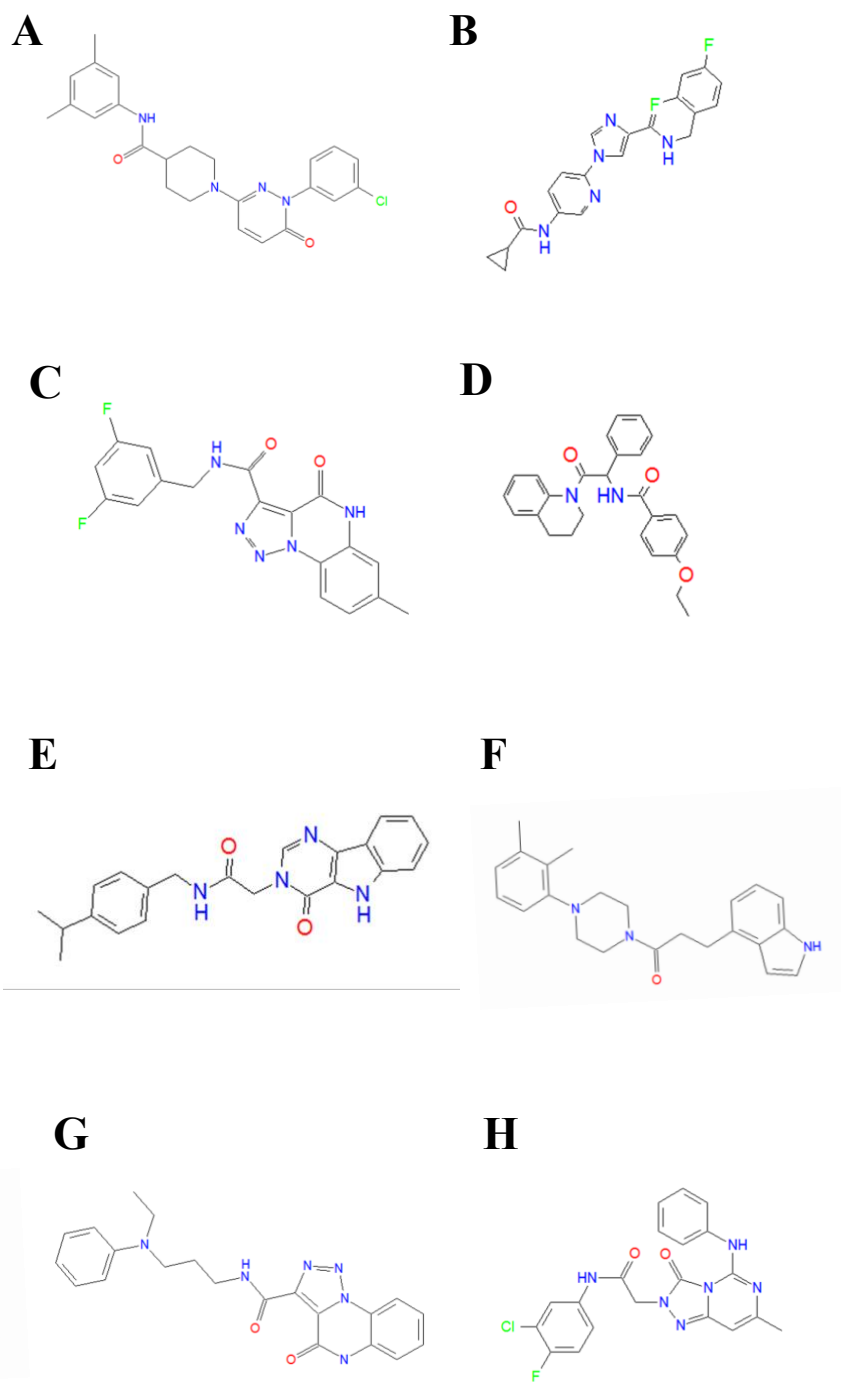


**Figure 19:** Structures of confirmed hit compounds that inhibit enzymatic activity of PaGluRS.

A) BCD36C3; B) BCD41A6; C) BCD47F11 D) BCD38E7; E) BCD36B4; F) BCD43A8; G) BCD47G7; H) BCD48B7

## Testing Compounds against PaPheRS, SpPheRS, and PaAspRS

Fifty-two compounds designed to inhibit PheRS were titrated into aminoacylation assays to determine  $IC_{50}$  values for dose response against PheRS from *P. aeruginosa* and *S. pneumoniae*. Six of the compounds were shown to have inhibitory activity, however  $IC_{50}$  values were very high, making the compounds unlikely prospects. Similarly, of the 29 compounds tested against *P. aeruginosa* AspRS, only three were observed to have inhibitory activity and the  $IC_{50}$  values were also very high.

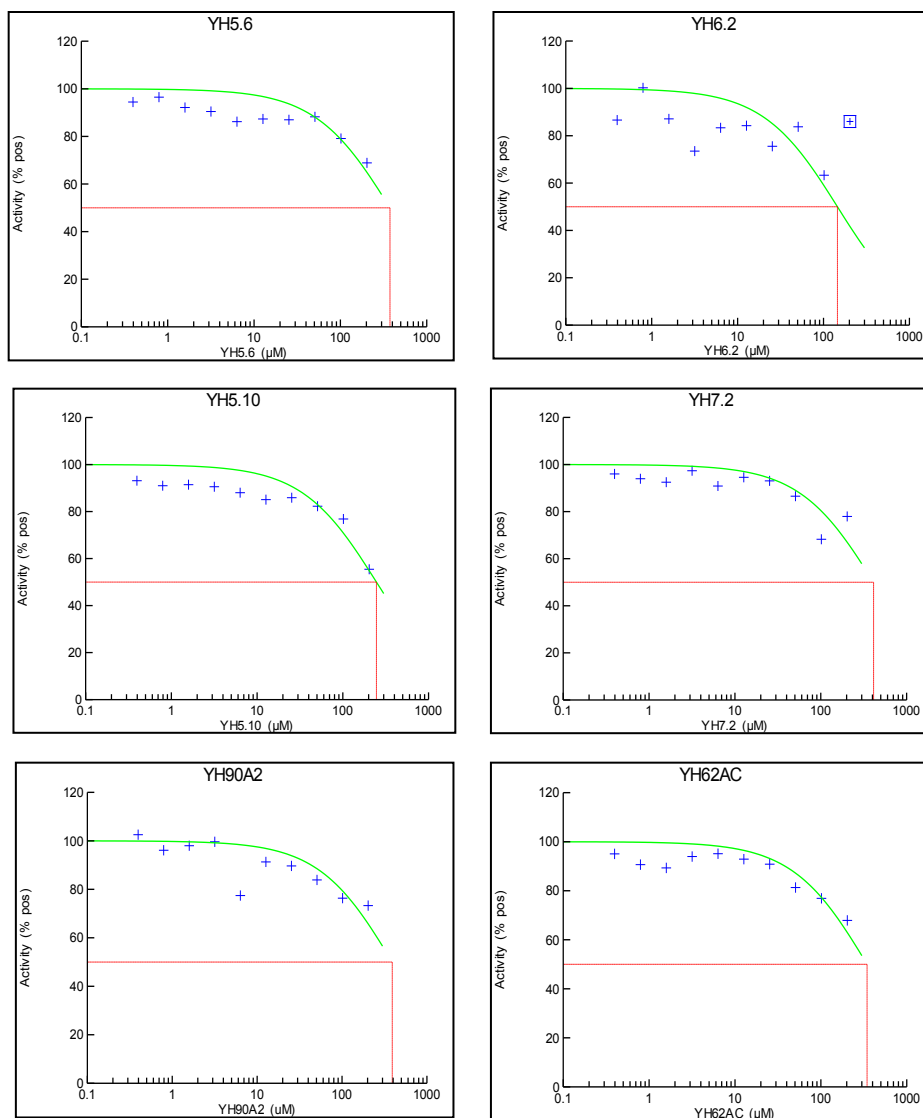


**Figure 20:**  $IC_{50}$  plots of compounds against the activity of SpPheRS

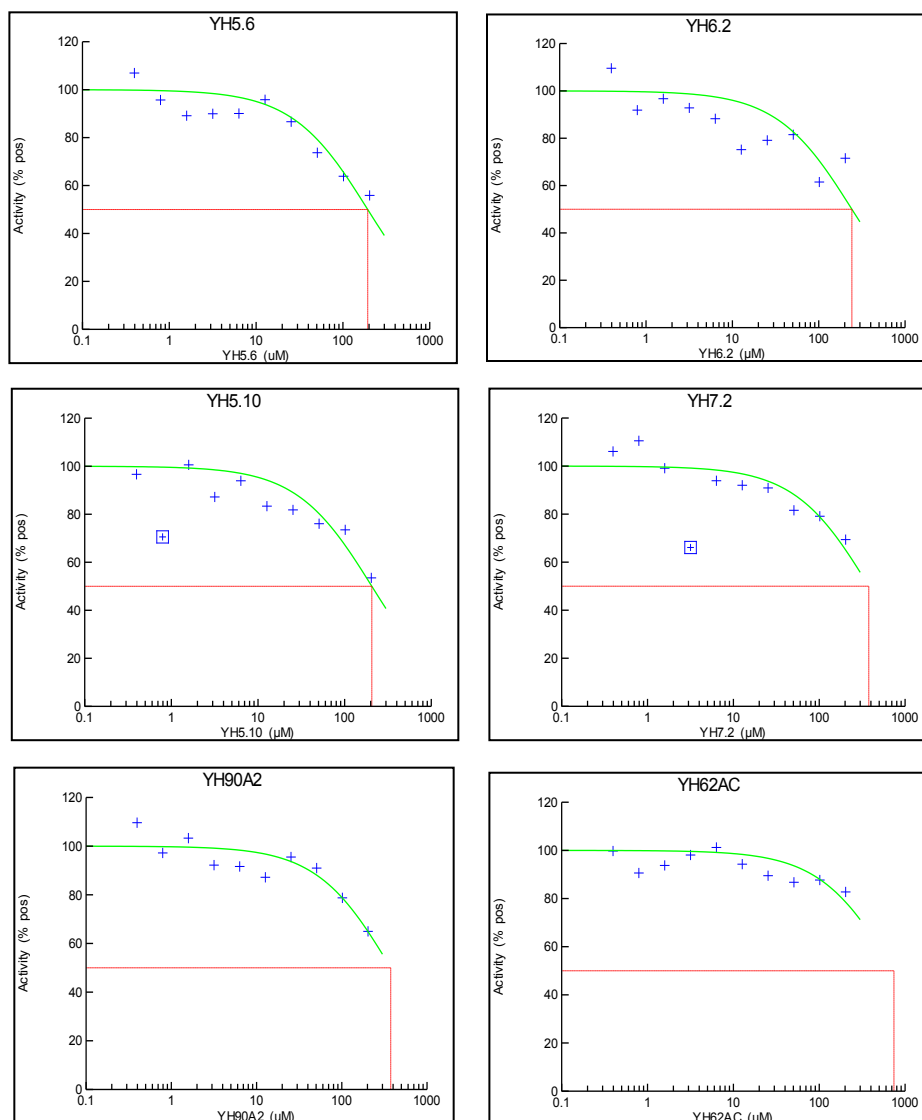


**Figure 21:** IC<sub>50</sub> plots of compounds against the activity of PaPheRS

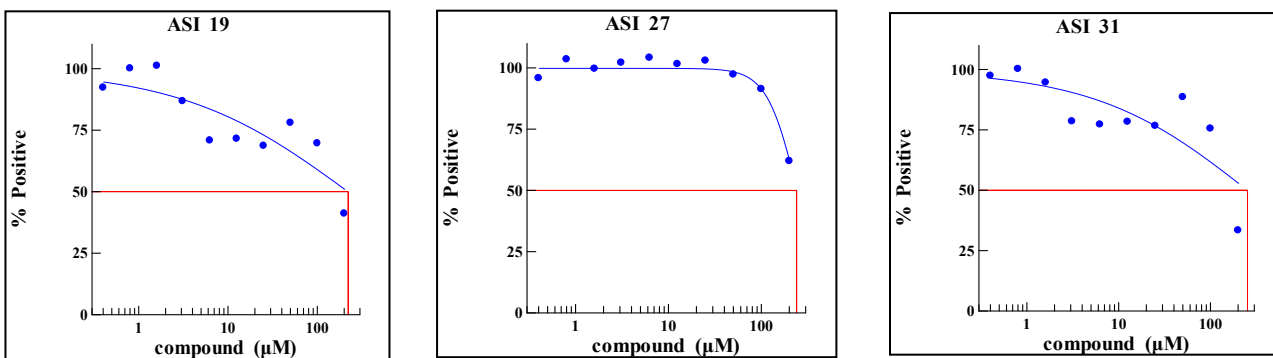


**Figure 22:** IC<sub>50</sub> plots of compounds against the activity of PaAspRS

### Testing the Amino Acid Peptide against Protein Synthesis System

The peptide that mimicked a region of IF-1 was tested against a polyU mRNA-directed aminoacylation/translation (A/T) assay. The peptide was designed to block IF-1 from binding to the ribosome. When tested against the A/T assay, the activity was affected by the addition of the peptide, showing that the peptide has promise as an enzymatic inhibitor of *P. aeruginosa*.

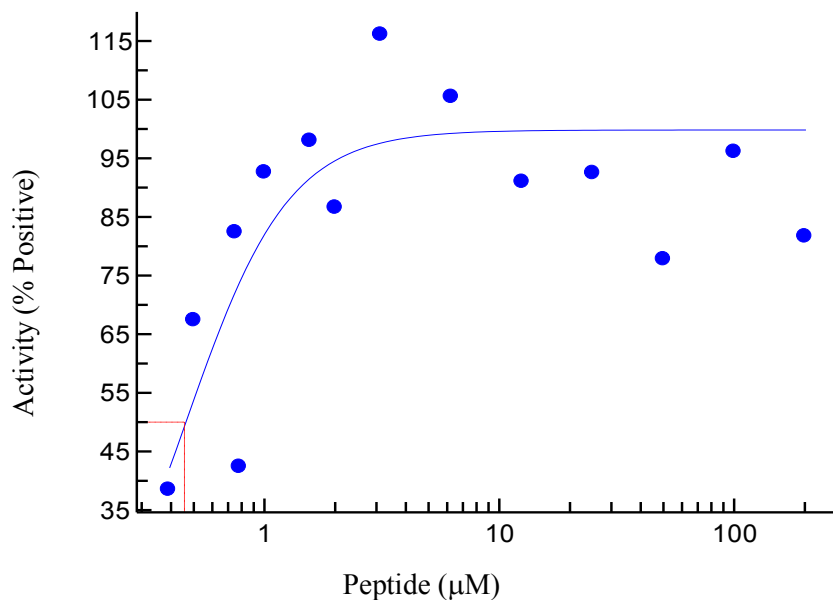


**Figure 23:** Titration of the IF-1 peptide mimic into the aminoacylation/translation assay.

## CHAPTER IV

### CONCLUSION

PaTyrRS-Z and PaTyrRS-S were cloned, overexpressed in *E. coli*, and purified to greater than 95% homogeneity. ATP:PP<sub>i</sub> exchange assays and aminoacylation assays were used to determine the kinetic parameters governing the interactions with ATP, tyrosine, and tRNA for each enzyme. Screening platforms for PaTyrRS-Z and PaTyrRS-S were developed and used to screen the ChemDiv Soluble Diversity Library (2000 compounds). After screening the library with PaTyrRS-Z, 10 initial hits were determined, and 1 compound confirmed to have inhibitory activity. This compound (BCD38C11) was titrated and the resulting IC<sub>50</sub> value was 269 μM. After screening the chemical compound library against the activity of PaTyrRS-S, 30 initial hits were determined and 10 were confirmed to have inhibitory activity. Five of these ten compounds were used in IC<sub>50</sub> assays (BCD37H, BCD38C11, BCD49D09, BCD50C03 and BCD54B04) and the resulting IC<sub>50</sub> values were 23.68, 57.59, 65.9, 34.41 and 44.31 μM respectively.

PaGluRS was also used to screen the ChemDiv Soluble Diversity Library. After screening with this enzyme, 32 initial hits were determined and 17 were confirmed to have inhibitory activity. After structural analysis, eight compounds were selected for additional analysis.

A total of 81 compounds were tested from Dr. Claire Simon's laboratory. Fifty-two compounds were tested against PaPheRS and SpPheRS and six were identified to have inhibitory activity. Twenty-nine compounds were tested against PaAspRS and three showed inhibition of

the system. Although titrated compounds showed a dose response,  $IC_{50}$  values were high, so these compounds are unlikely candidates for antibiotic therapy.

The peptide from Dr. Zhang's laboratory was tested against an aminoacylation/translation assay. Since the peptide titrated and showed a dose response, it appeared to relieve the IF-1 induced inhibition of initiation of protein synthesis in *P. aeruginosa* and may have potential as an antimicrobial therapeutic.



## REFERENCES

1. Centers for Disease Control and Prevention (CDC): Antibiotic resistance threats in the United States, 2013. *Medical Benefits* 2014, 31(1):12.
2. Ventola CL: The Antibiotic Resistance Crisis: Part 1: Causes and Threats. *P & T: a peer-reviewed journal for formulary management* 2015, 40(4):277.
3. Tenover FC: Mechanisms of Antimicrobial Resistance in Bacteria. *Am J Med* 2006, 119(6):S10.
4. Nathwani D, Raman G, Sulham K, Gavaghan M, Menon V: Clinical and economic consequences of hospital-acquired resistant and multidrug-resistant *Pseudomonas aeruginosa* infections: a systematic review and meta-analysis. *Antimicrobial resistance and infection control* 2014, 3(1):32.
5. Shrivastava S, Shrivastava P, Ramasamy J: World health organization releases global priority list of antibiotic-resistant bacteria to guide research, discovery, and development of new antibiotics. *Journal of Medical Society* 2018, 32(1):76.
6. Mah TC, O'Toole GA: Mechanisms of biofilm resistance to antimicrobial agents. *Trends in Microbiology* 2001, 9(1):34-39.
7. Palmer GC, Whiteley M: Metabolism and Pathogenicity of *Pseudomonas aeruginosa* Infections in the Lungs of Individuals with Cystic Fibrosis. *Microbiology Spectrum* 2015, 3(4).
8. Spellberg B, Guidos R, Gilbert D, Bradley J, Boucher HW, Scheld WM, Bartlett JG, Edwards J, Jr, the Infectious Diseases Society of America: The Epidemic of Antibiotic-Resistant Infections: A Call to Action for the Medical Community from the Infectious Diseases Society of America. *cid* 2008, 46(2):155-164.
9. Schäberle, Till F. Hack, Ingrid M: Overcoming the current deadlock in antibiotic research. *Trends in Microbiology* 2013, 22(4):165-167.
10. Cabot G, Zamorano L, Moyà B, Juan C, Navas A, Blázquez J, Oliver A: Evolution of *Pseudomonas aeruginosa* Antimicrobial Resistance and Fitness under Low and High Mutation Rates. *Antimicrobial agents and chemotherapy* 2016, 60(3):1767-1778.

11. Machado I, Coquet L, Jouenne T, Pereira MO: Proteomic approach to *Pseudomonas aeruginosa* adaptive resistance to benzalkonium chloride. *Journal of Proteomics* 2013, 89:273-279.
12. Poole K: Efflux pumps as antimicrobial resistance mechanisms. *Annals of Medicine* 2007, 39(3):162-176.
13. Blanco P, Hernando-Amado S, Reales-Calderon JA, Corona F, Lira F, Alcalde-Rico M, Bernardini A, Sanchez MB, Martinez JL: Bacterial Multidrug Efflux Pumps: Much More Than Antibiotic Resistance Determinants. *Microorganisms* 2016, 4(1):14.
14. Poole K: *Pseudomonas aeruginosa*: resistance to the max. *Frontiers in microbiology* 2011, 2:65.
15. Olga Lomovskaya, Mark S. Warren, Angela Lee, Jorge Galazzo, Richard Fronko, May Lee, Johanne Blais, Deidre Cho, Suzanne Chamberland, Tom Renau, Roger Leger, Scott Hecker, Will Watkins, Kazuki Hoshino, Hiroko Ishida, Ving J. Lee: Identification and Characterization of Inhibitors of Multidrug Resistance Efflux Pumps in *Pseudomonas aeruginosa*: Novel Agents for Combination Therapy. *Antimicrobial Agents and Chemotherapy* 2001, 45(1):105-116.
16. Rampioni G, Pillai CR, Longo F, Bondi R, Baldelli V, Messina M, Imperi F, Visca P, Leoni L: Effect of efflux pump inhibition on *Pseudomonas aeruginosa* transcriptome and virulence. *Scientific reports* 2017, 7(1):11392-14.
17. Li Zhang, Xian-Zhi Li, Keith Poole: Fluoroquinolone susceptibilities of efflux-mediated multidrug-resistant *Pseudomonas aeruginosa*, *Stenotrophomonas maltophilia* and *Burkholderia cepacia*. *The Journal of Antimicrobial Chemotherapy* 2001, 48(4):549-552.
18. Wolter DJ, Smith-Moland E, Goering RV, Hanson ND, Lister PD: Multidrug resistance associated with mexXY expression in clinical isolates of *Pseudomonas aeruginosa* from a Texas hospital. *Diagnostic Microbiology and Infectious Disease* 2004, 50(1):43-50.
19. D G Thanassi, G S Suh, H Nikaido: Role of outer membrane barrier in efflux-mediated tetracycline resistance of *Escherichia coli*. *Journal of Bacteriology* 1995, 177(4):998-1007.
20. Hiroshi Nikaido, Marti Vaara Department Microbiology Immunology, University of California, Berkeley, California 9, 1 N P Health I, SF-00280 Helsinki, Finland2: Molecular Basis of Bacterial Outer Membrane Permeability. 1985, 49.
21. Strateva T, Yordanov D: *Pseudomonas aeruginosa* - a phenomenon of bacterial resistance. *Journal of Medical Microbiology* 2009, 58(9):1133-1148.
22. Higgins PG, Fluit AC, Schmitz FJ: Fluoroquinolones: Structure and Target Sites. Bentham Science Publishers 2013, 4(2):190(10).

23. Wolter DJ, Lister PP: Mechanisms of  $\beta$ -lactam Resistance Among *Pseudomonas aeruginosa*. *Current Pharmaceutical Design* 2013, 19(209).
24. Poole K: Outer Membranes and Efflux: The Path to Multidrug Resistance in Gram- Negative Bacteria; *Current Pharmaceutical Biotechnology* 2002, 3(77).
25. Bush K, Bradford P:  *$\beta$ -Lactams and  $\beta$ -Lactamase Inhibitors: An Overview*; 2016.
26. Meletis G: Carbapenem resistance: overview of the problem and future perspectives. *Therapeutic Advances in Infectious Disease* 2016, 3(1):15-21.
27. John Quale, Simona Bratu, Jyoti Gupta, David Landman: Interplay of Efflux System, ampC, and oprD Expression in Carbapenem Resistance of *Pseudomonas aeruginosa* Clinical Isolates. *Antimicrobial Agents and Chemotherapy* 2006, 50(5):1633-1641.
28. Labby KJ, Garneau-Tsodikova S: Strategies to overcome the action of aminoglycoside-modifying enzymes for treating resistant bacterial infections. *Future Medicinal Chemistry* 2013, 5(11):1285-1309.
29. Vázquez-Espinosa E, Girón RM, Gómez-Punter RM, García-Castillo E, Valenzuela C, Cisneros C, Zamora E, García-Pérez FJ, Ancochea J: Long-term safety and efficacy of tobramycin in the management of cystic fibrosis. *Therapeutics and clinical risk management* 2015, 11:407-415.
30. Hurdle JG, O'Neill AJ, Chopra I: Prospects for Aminoacyl-tRNA Synthetase Inhibitors as New Antimicrobial Agents. *Antimicrobial agents and chemotherapy* 2005, 49(12):4821-4833.
31. Tan M, Wang M, Zhou X, Yan W, Eriani G, Wang E: The Yin and Yang of tRNA: proper binding of acceptor end determines the catalytic balance of editing and aminoacylation. *Nucleic acids research* 2013, 41(10):5513-5523.
32. Salazar JC, Zuñiga R, Lefimil C, Söll D, Orellana O: Conserved amino acids near the carboxy terminus of bacterial tyrosyl-tRNA synthetase are involved in tRNA and Tyr-AMP binding. *FEBS Letters* 2001, 491(3):257-260.
33. Bullwinkle TJ, Ibba M: Emergence and Evolution. *Topics in current chemistry* 2014, 344:43.
34. Berg JM, Tymoczko JL, Stryer L: Section 29.2, Aminoacyl-Transfer RNA Synthetases Read the Genetic Code. In *Biochemistry*. 5th edition. Edited by Anonymous New York: WH Freeman; 2002.
35. Glickman JF, Schmid A, Ferrand S: Scintillation Proximity Assays in High-Throughput Screening. *ASSAY and Drug Development Technologies* 2008, 6(3):433-455.

36. Macarrón R, Mensah L, Cid C, Carranza C, Benson N, Pope AJ, Díez E: A Homogeneous Method to Measure Aminoacyl-tRNA Synthetase Aminoacylation Activity Using Scintillation Proximity Assay Technology. *Analytical Biochemistry* 2000, 284(2):183-190.
37. Zhang L, Gallo RL: Antimicrobial peptides. *Current Biology* 2016, 26(1):R19.
38. Hu Y, Keniry M, Palmer SO, Bullard JM: Discovery and Analysis of Natural-Product Compounds Inhibiting Protein Synthesis in *Pseudomonas aeruginosa*. *Antimicrobial agents and chemotherapy* 2016, 60(8):4820-4829.
39. Cull MG, McHenry CS: Purification of Escherichia coli DNA polymerase III holoenzyme. In *Methods in Enzymology. Volume 262*. Edited by Anonymous United States: Elsevier Science & Technology; 1995:22-35.
40. Hu Y, Palmer SO, Munoz H, Bullard JM: High Throughput Screen Identifies Natural Product Inhibitor of Phenylalanyl-tRNA Synthetase from *Pseudomonas aeruginosa* and *Streptococcus pneumoniae*. *Current drug discovery technologies* 2014, 11(4):279.
41. Palmer SO, Hu Y, Keniry M, Bullard JM: Identification of Chemical Compounds That Inhibit Protein Synthesis in *Pseudomonas aeruginosa*. *SLAS Discovery* 2017, 22(6):775-782.

## BIOGRAPHICAL SKETCH

The author, Casey Anne Hughes (casey.hughes01@utrgv.edu, kkhugs@gmail.com, or caseyanneleo@yahoo.com) was born in Harlingen, Texas on September 6, 1994. She graduated from the University of Texas Rio Grande Valley (UTRGV) with a Bachelor of Science degree in Biology with a minor in Chemistry in the summer of 2017. In the fall of 2017, Casey joined the UTRGV graduate program in Chemistry and graduated with her Master of Science degree in the spring of 2019.